2016

Flying under the LiDAR: relating forest structure to bat community diversity

Anna Schneider Swanson
University of Central Florida

FLYING UNDER THE LiDAR:
RELATING FOREST STRUCTURE TO BAT COMMUNITY DIVERSITY

by

ANNA CHRISTINE SCHNEIDER SWANSON
B.S. University of Central Florida, 2012
M.A.T. University of Central Florida, 2013

A thesis submitted in partial fulfillment of the requirements
for the degree of Master of Science
in the Department of Biology
in the College of Sciences
at the University of Central Florida
Orlando, Florida

Spring Term
2016

Major Professor: John F. Weishampel

ABSTRACT

Bats are important to many ecological processes such as pollination, insect (and by proxy, disease) control, and seed dispersal and can be used to monitor ecosystem health. However, they are facing unprecedented extinction risks from habitat degradation as well as pressures from pathogens (e.g., white-nose syndrome) and wind turbines. LiDAR allows ecologists to measure structural variables of forested landscapes with increased precision and accuracy at broader spatial scales than previously possible. This study used airborne LiDAR to classify forest habitat/canopy structure at the Ordway-Swisher Biological Station (OSBS) in north central Florida. LiDAR data were acquired by the National Ecological Observatory Network (NEON) airborne observation platform in summer 2014. OSBS consists of open-canopy pine savannas, closed-canopy hardwood hammocks, and seasonally inundated basin marshes. Multiple forest structural parameters (e.g., mean, maximum, and standard deviation of canopy height) were derived from LiDAR point clouds using the USDA software program FUSION. K-means clustering was used to segregate each 5x5 m raster across the ~3765 ha OSBS area into six different clusters based on the derived canopy metrics. Cluster averages for maximum, mean, and standard deviation of return heights ranged from 0 to 19.4 m, 0 to 15.3 m, and 0 to 3.0 m, respectively. To determine the relationships among these landscape-canopy features and bat species diversity and abundances, AnaBat II bat detectors were deployed from May to September in 2015 stratified by these distinct clusters. A statistical regression model selection approach was performed in order to evaluate how forest structural attributes such as understory clutter, vertical canopy structure, open and closed canopy, etc. and landscape metrics influence bat communities. The most informative models showed that a combination of site-specific (e.g., midstory clutter and entropy) and landscape level attributes (e.g., area of water and service road length) contributed to bat community patterns. This knowledge provides a deeper understanding of habitat-species interactions to better manage survival of these species and provides insight into new tools for landscape management as they apply to specific species

ACKNOWLEDGMENTS

I would like to thank my advisor, Dr. John Weishampel, for all of the guidance he has given me during this project. It would not have been possible without all of the work he put in to help me through the thesis. In addition, my committee members, Dr. Reed Noss and Dr. Josh King, also provided invaluable feedback which greatly improved this project. I am grateful to both Dr. Pedro Quintana-Ascencio and Dr. David Jenkins for comments on experimental design and for help with statistical analysis. This project could not have been completed without the help of Laura Finn and Fly By Night, Inc. who provided the bat detectors and expert advice on the bats of central Florida. Dr. Bruce Miller also helped with acoustic identification of bats. Stephen Coates and the staff at Ordway-Swisher Biological Station deserve my gratitude for rescuing me on more than one occasion and also for the support throughout this project. Finally, I would like to thank my field assistants, Kevin Mayer, Regan Schwartz, Tom Swanson, and Charles Wayne, who spent their summer helping me with equipment setup in spite of oppressive heat, rain, and myriad ticks. LiDAR was collected by NEON, Inc. The National Observatory Network is a project sponsored by the National Science Foundation and managed under cooperative agreement by NEON, Inc. This material is based in part upon work supported by the National Science Foundation under Grant No. DBI-0752017. Additional funding for this project was provided by the Learning Institute for Elders (LIFE) at UCF.

TABLE OF CONTENTS

LIST OF FIGURES vii

LIST OF TABLES viii

LIST OF ACRONYMS x

INTRODUCTION 1

METHODOLOGY 5

Study Location 5

Site Selection for Acoustic Sampling 6

Detector Setup 7

Data Analysis 8

RESULTS 14

K Means Clustering 14

Acoustics Summary 17

Model Selection 20

DISCUSSION 27

APPENDIX A: CORRELATION MATRICES 31

APPENDIX B: SITE AND MODEL SELECTION PARAMETERS 67

APPENDIX C: SAMPLING TIMES 70

APPENDIX D: COMPLETE MODEL SELECTION RESULTS 72

APPENDIX E: R CODE 77

Correlation Matrices 78

K Means Clustering and Site Selection 78

Model Selection 80

APPENDIX F: IACUC APPROVAL 90

LIST OF REFERENCES 93

LIST OF FIGURES

Figure 1: Differences in foraging strategy and frequency of calls are related. Bats that forage in open areas (1, 2, 5, 6) have lower frequency calls while those that forage in cluttered areas (3, 4) have higher frequency calls (from Aldridge and Rautenbach 1987). 3

Figure 2: Wing loading and aspect ratio of bats of north central Florida, based on Farney and Fleharty (1969); acronyms are the combined first two letters of the genus and species name. Species in red are my predictions based on photographs and foraging behavior. 6

Figure 3: A) OSBS 5 x 5 m k-means cluster results; B) vegetative communities at OSBS as defined by Florida Natural Areas Inventory (FNAI) 10

Figure 4: Level 1 FLUCCS designations for 1.5 km buffer around OSBS 11

Figure 5: Cluster metrics for A) canopy mean and B) rugosity. Colors correspond to clusters from Figure 3A. The line within the boxplot is the median while the circles are outliers outside of one standard deviation from the mean. 15

Figure 6: LiDAR point clouds for representative sites at each cluster; the radius of the ground surface (blue disk) is 12.5 m. 16

Figure 7: Total bat abundance by site; sites are color coded by cluster corresponding with Figure 3A. The line through the boxes represents the median while open circles are outlier points. 17

Figure 8: Jost bat diversity for each site; colors correspond to the clusters from Figure 3A. The line through the boxes represents the median while open circles are outlier points. 18

Figure 9: Species accumulation curves per cluster which are represented by different colored lines based on Figure 3A. EchoClass v 3.1 had the ability to identify 7 total species. 19

LIST OF TABLES

Table 1: Final parameters used in models selection and their ecological significance 12

Table 2: Parameters for numbered models. 13

Table 3: Results for most informative total abundance model. 20

Table 4: Results for second most informative total abundance model. 21

Table 5: Results for third most informative total abundance model. 21

Table 6: Results for most informative community diversity model. 22

Table 7: Results for most informative logistic model, evening bat (*N. humeralis*). 23

Table 8: Results for most informative logistic model, tricolored bat (*P. subflavus*). 24

Table 9: Results for most informative logistic model, southeastern myotis (*M. austroriparius*). 25

Table 10: Results for most informative logistic model, big brown bat (*E. fuscus*). 26

Table A1: Correlation matrix of LiDAR parameters for k-means clustering (extends through page 65); blue cells are positively related and red cells are negatively related. ND values represent no 32

Table A2: Correlation matrix of potential model parameters. 66

Table B1: Site selection parameters for k-means clustering analysis. 68

Table B2: Complete parameter set for model development. 69

Table C1: Sampling weeks for each site (cluster 1 - red, 2 - orange, 3 - yellow, 4 - purple, 5 - blue, 6 - green) corresponding to Figure 3A. 71

Table D1: AIC table for bat abundance models. 73

Table D2: AIC table for bat community diversity models. 73

Table D3: AIC table for logistic models, evening bat (*N. humeralis).* 74

Table D4: AIC table for logistic models, tricolored bat (*P. subflavus).* 74

Table D5: AIC table for logistic models, southeastern myotis (*M austroriparius).* 75

Table D6: AIC table for logistic models, big brown bat (*E. fuscus).* 75

Table D7: Results for second most informative logistic model, big brown bat (*E. fuscus*)..... 76

Table D8: Results for third most informative logistic model, big brown bat (*E. fuscus*). 76

LIST OF ACRONYMS

AICc: Akaike's Information Criterion for small sample sizes

ALTM: airborne laser terrain mapping

CF: Compact Flash

CORA: *Corynorhynus rafinesquii*, Rafinesque's big-eared bat

EPFU: *Eptesicus fuscus*, big brown bat

FLUCCS: Florida Land Use, Cover and Forms Classification System

FNAI: Florida Natural Areas Inventory

GLM: Generalized Linear Model

LABO: *Lasiurus borealis*, eastern red bat

LACI: *Lasiurus cinerius*, hoary bats

LAIN: *Lasiurus intermedius*, northern yellow bat

LASE: *Lasiurus seminolus*, Seminole bat

LiDAR: light detection and ranging

LTK: LiDAR Toolkit

MYAU: *Myotis austroriparius*, southeastern myotis

NEON: National Ecological Observatory Network

NYHU: *Nycticeius humeralis*, evening bat

OSBS: Ordway-Swisher Biological Station

PESU: *Perimyotis subflavus*, tricolored bat

TABR: *Tadarida brasilienses*, Mexican free-tailed bat

USDA: United States Department of Agriculture

ZCAIM: Zero-Crossings Analysis Interface Module

INTRODUCTION

Understanding the drivers of biodiversity is essential for species conservation. The habitat heterogeneity hypothesis (Lack, 1969, MacArthur and Wilson, 1967) posits that as areas increase in structural complexity, additional niches are opened for exploitation, therefore allowing diversification of species that used these varied niches. MacArthur (1958) was one of the first researchers to notice this diversification in birds based on vertical heterogeneity of forest structure. In a later study, MacArthur and MacArthur (1961) developed the foliage height diversity index which classified forests based on percentage of leaf area within different height classes. With this measurement approach, forests were more structurally diverse if they had an even distribution of leaf area throughout the different canopy layers (higher entropy) or less structurally diverse if they had uneven distribution of leaf area throughout the different canopy layers (lower entropy). Following these studies, many other researchers explored the positive relationship between vertical habitat heterogeneity and increased diversity in primates (Schwarzkopf and Rylands, 1989), birds (Bersier and Meyer, 1994), spiders (Docherty and Leather, 1997), macropods (Southwell, Cairns, Pople *et al.*, 1999), arboreal arthropods (Halaj, Ross and Moldenke, 2000), ants (Bestelmeyer and Wiens, 2001), and amphibians (Vallan, 2002).

Bats represent greater than 20% of all mammalian diversity worldwide (Mickelburg, Hutson and Racey, 2002) and play important roles in forested ecosystems by acting as pollinators, seed dispersers, and insect predators, which provides top-down control to reduce herbivory within ecosystems (Bohm, Wells and Kalko, 2011). It has also been suggested that bats serve as good bioindicators (Jones, Jacobs, Kunz *et al.*, 2009) to monitor environmental degradation and decline in biodiversity (Waldon, Miller and Miller, 2011). Bats also play a role in cycling nutrients through the forest, possibly even acting as a primary nutritional support for

guano-dependent plants near their roosts (Duchamp, Sparks and Swihart, 2010). However, bat species throughout the world are in decline (Mickleburgh, Hutson and Racey, 2002) due to environmental stressors such as habitat loss and fragmentation, white nose syndrome (Frick, Pollock, Hicks *et al.*, 2010), and increased use of wind turbines (Arnett, Brown, Erickson *et al.*, 2008).

The wing morphology of bats informs us about a bat's foraging strategy. Bats that forage in more open areas are adapted for faster flight and therefore have higher mass, wing loading (weight of the bat divided by the total area of the wing), and aspect ratio (wing span of the bat squared divided by the wing area) (Aldridge and Rautenbach, 1987). On the other hand, bats that forage in densely vegetated areas tend to be smaller and adapted for slower, more maneuverable flight with low wing loading and aspect ratio (Aldridge and Rautenbach, 1987). Bat echolocation is a part of the same adaptive complex (Aldridge and Rautenbach, 1987), so bats that forage within densely forested patches have different foraging calls from those that forage in open areas. To forage efficiently in areas with high three-dimensional complexity, or vegetative clutter, bats evolved mechanisms which allow them to segregate vegetative clutter from potential prey while also maintaining the ability to properly orient themselves and avoid obstacles (Schnitzler and Kalko, 2001). Figure 1 shows differentiation in foraging strategy and echolocation frequency (kHz) of forest-dwelling bats.

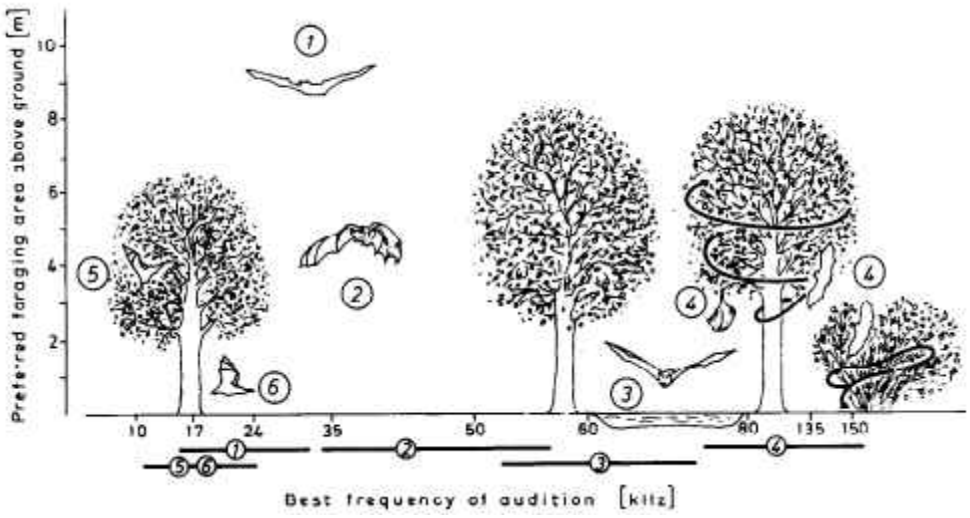

Figure 1: Differences in foraging strategy and frequency of calls are related. Bats that forage in open areas (1, 2, 5, 6) have lower frequency calls while those that forage in cluttered areas (3, 4) have higher frequency calls (from Aldridge and Rautenbach 1987).

Loeb and O'Keefe (2006) determined that in addition to forest stand-level characteristics, landscape parameters also play a role in foraging use of an area by bats. Measures of landscape heterogeneity are difficult to quantify in the field. One form of remote sensing, LiDAR (light detection and ranging), allows ecologists to quickly and accurately measure forest structural parameters across large tracts (Lefsky, Cohen, Parker *et al.*, 2002). Many forest variables such as canopy height, canopy cover/closure, and vertical distribution of canopy cover (entropy) can be derived either directly or indirectly from LiDAR returns (Merrick, Koprowski and Wilcox, 2012)

LiDAR systems map forest structure by emitting laser pulses from a known position and measuring the amount of time it takes for the photons to travel back to the mounted receiver (Reutebuch, Andersen and McGaughey, 2005). The first pulses to return represent the canopy top while the last returns represent the ground. Returns in the middle represent the vertical heterogeneity of the forest (i.e., understory, mid-canopy, etc.). Airborne LiDAR systems are capable of mapping out large areas of land by sending out tens of thousands of laser pulses per

second (Reutebuch *et al.*, 2005). These pulses are represented in a point cloud, a 3-dimensional map of surfaces with x, y, and z spatial locations. Forest metrics such as canopy height (first return – last return), rugosity (standard deviation of canopy height), and canopy cover measurements which are derived by measuring the proportion of ground returns that are received by a sensor (Lefsky *et al.*, 2002) can be derived from the LiDAR point cloud.

The ability to measure canopy metrics at large scales has spurred a variety of studies on the relationships between forest canopy structure and community composition of different taxa (Davies and Asner, 2014) including spiders (Vierling, Bassler, Brandl *et al.*, 2011), birds (Clawges, Vierling, Vierling *et al.*, 2008, Goetz, Steinberg, Dubayah *et al.*, 2007), beetles (Muller and Brandl, 2009), other arthropods (Müller, Bae, Röder *et al.*, 2014), and primates (Palminteri, Powell, Asner *et al.*, 2012). A study by Jung, Kaiser, Bohm et al. (2012) looked at how management practices affecting three-dimensional forest structure influence insectivorous bat community composition. My study combines the approaches of Jung et al. (2012) and Loeb and O'Keefe (2006) to investigate how LiDAR-derived forest structure parameters at the patch scale and landscape-level attributes (such as road density and landscape heterogeneity) relate to bat abundance, bat community diversity, and use of sites by individual bat species across a heterogeneous landscape in north central Florida. This study is the first to examine the relationship of LiDAR-derived canopy structure to bat species and assemblages in the Western Hemisphere. In addition to quantifying relationships among individual landscape and site-specific parameters, it will also examine whether the interactions of these effects are important to these population-level and community-level measures.

METHODOLOGY

Study Location

The study was conducted at the Ordway-Swisher Biological Station (OSBS) in Melrose, Florida (29.68° N and 82.00° W). The station is approximately 3765 ha and is operated by the University of Florida as a research station. This site is also part of the National Ecological Observatory Network (NEON), which gathers data for long term ecological monitoring and forecasting at various sites throughout the United States. Vegetative communities at OSBS include sandhills, xeric hammocks, upland mixed forests, swamps, and marshes. To maintain natural disturbance regimes, the pyrogenic communities are managed with prescribed fire with between 690 and 810 ha burned annually (Ordway-Swisher Biological Station, 2014). Since the 1930s the land was used as a private hunting and fishing preserve and by the 1980s much of the land had been set aside for conservation and research. The relatively long history of conservation at OSBS makes it an ideal study site as the natural floral and faunal communities have been given time to recuperate from human influence. The large size of the station can act as a buffer against impact from the human matrix outside.

Based on geographic ranges, ten different species of bats are expected to reside within OSBS: Rafineque's big-eared bat (*Corynorhinus rafinesquii*, CORA), big brown bat (*Eptesicus fuscus*, EPFU), eastern red bat (*Lasiurus borealis,* LABO), hoary bat (*L. cinerius*, LACI), northern yellow bat (*L. intermedius*, LAIN), Seminole bat (*L. seminolus*, LASE), southeastern myotis (*Myotis austroriparius*, MYAU), evening bat (*Nyctecius humeralis*, NYHU), tricolored bat (*Perimyotis subflavus*, PESU), and the Mexican free-tailed bat (*Tadarida brasilienses*, TABR) (Marks and Marks 2006). *P. subflavus* is a clutter tolerant bat, *L. borealis* is semi clutter tolerant, and *L. cinereus* and *T. brasilienses* are clutter intolerant (Farney and Fleharty, 1969). Figure 2 shows wing loading and aspect ratios for several bat species of central Florida.

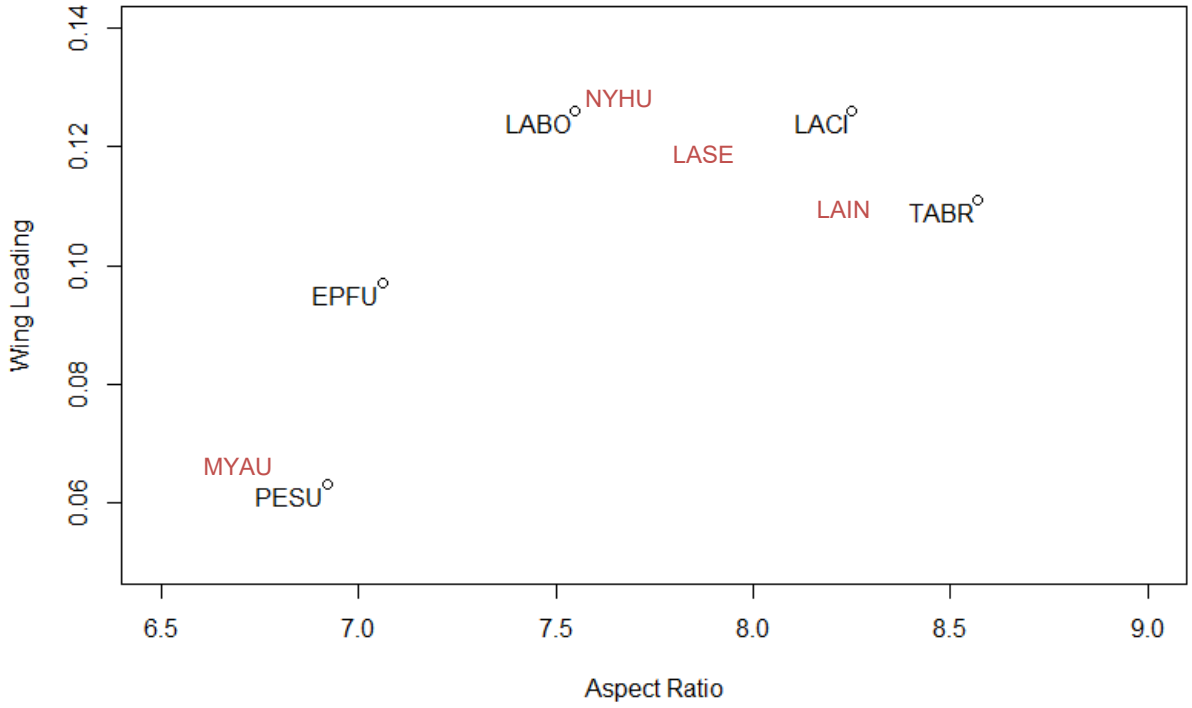

Figure 2: Wing loading and aspect ratio of bats of north central Florida, based on Farney and Fleharty (1969); acronyms are the combined first two letters of the genus and species name. Species in red are my predictions based on photographs and foraging behavior.

Site Selection for Acoustic Sampling

LiDAR data were acquired for OSBS by the NEON airborne observation platform on June 5, 2014. An Optech Gemini ALTM (airborne laser terrain mapping) sensor was flown onboard a Twin Otter aircraft. The LiDAR point density was approximately 3 points/m^2. To select sites that were appropriate for LiDAR analysis and to minimize impacts of variables that were not of interest, 50m buffers around roads, lakes, and the property perimeter were removed from the larger dataset. The LiDAR data were subdivided in to a 5 x 5 m grid. This scale was chosen because detectability of bat calls with AnaBat detectors drops off greatly after 5 m. (Adams, Jantzen, Hamilton *et al.*, 2012). Batch processing of LiDAR files was done in the USDA's LTKProcessing v. 1.0 program (McGaughey, 2014). This program

calculated 66 different parameters from the LiDAR point cloud data, some of which were either deemed unrelated to the study or else were highly correlated to other measured parameters.

A correlation analysis was performed to identify parameters that were highly correlated. Parameters that had a 75% or greater positive or negative correlation to other parameters were eliminated based on relevance to the study questions (Appendix A, Table A1). Parameters that were considered particularly relevant to bat species occurrence were kept in the model even if they correlated highly with other parameters. These decisions were based largely on the Jung et al. (2012) study.

Based on these criteria, 14 parameters (Appendix B, Table B1) were chosen to perform a k-means clustering analysis to partition OSBS into areas which had similar structural components. Six clusters were isolated representing a range from basin marshes to closed-canopy hardwood hammock. Figure 3 shows the resulting k-means cluster raster (A) along with vegetative communities (B).

After performing the k-means clustering analysis, 30 sites from each cluster were randomly selected by using the random function in R (R Development Core Team, 2014). These sites were brought into ArcGIS v. 10.1 (Environmental Systems Resource Institute, 2012). A 250 m buffer was placed around each site. Sites with overlapping buffers were removed to minimize spatial autocorrelation. Sites that were not representative of the area, i.e., they were surrounded by other cluster types, were also removed. Sites were further eliminated based on accessibility until eighteen sites remained - three from each cluster.

Detector Setup

Two sampling periods were conducted from June 16 through September 7, 2015. Each site was visited twice per week. The first visit was used to set up the AnaBat detectors in water resistant casing. Each detector was positioned on a tripod approximately 1.5 m above ground level (O'Farrell, 1998) and the microphone was pointed away from vegetation clutter. The tripod was tied to a tree or staked to the ground, and camouflage was placed around the water resistant container. To minimize variability between detectors, each was set to the same sensitivity. Nightly calls were recorded by a ZCAIM (zero-crossings

analysis interface module) unit plugged into the AnaBat detector with start time for recording delayed until 15 minutes before sunset to 15 minutes after sunrise. Three days after deploying the detectors, batteries in both the detectors and the ZCAIM unit were replaced. The goal was to have six consecutive nights of recorded calls. On the seventh day of the weekly cycle, detectors were removed from their locations and data were downloaded using CFCRead Storage ZCAIM Interface (Corben, 2014). Compact Flash (CF) cards were erased and replaced in the ZCAIM units. Detectors were transported to a new site. Which particular detector was used for a particular site was haphazardly determined. Table C1 in Appendix C shows the sampling times for each site.

Data Analysis

To create models which accurately represent parameters that affect site selection by bats at both the site and landscape level, several forest structure and landscape parameters were included in a multiple regression analysis. I calculated several landscape metrics within a 1.5 km buffer around each detector site. The 1.5 km radius was chosen as a low-end foraging distance from roosts (Henry, Thomas, Vaudry *et al.*, 2002, Hutchinson and Lacki, 2000). Within each buffer, level 1 Florida Land Use, Cover and forms Classification System (FLUCCS) codes were used to determine the proportion of urban, agricultural, forested and nonforested lands present (Figure 4). I also measured total length of service roads and area of standing water within each buffer. These measurements were derived from GIS layers created by OSBS managers. I measured landscape heterogeneity using Jost diversity (Jost, 2006) to determine the effective diversity of k-means cluster types within a given buffer. These measurements were limited to the perimeter of OSBS. Table B2 in Appendix B summarizes all of the parameters considered as well as their biological relevance. Analysis of the correlation matrix was performed to determine which variables should be removed to reduce collinearity in the models (Appendix A, Table A2). Final parameters used in the models are described in Table 1.

Due to limited familiarity with specific bat calls, I used the automated bat call identification software package, Echoclass v. 3.1 (Britzke, 2014). This software has been approved by the United States

Fish and Wildlife Service (USFWS) (U.S. Fish and Wildlife Service, 2015) for conducting Indiana bat (*Myotis sodalis*) surveys, and a test conducted on several automated bat identification software packages, including Echoclass, demonstrated that Echoclass correctly identified South Carolina bat species 72% of the time (Ford, 2014). However, 28% of calls were mis- or unidentified, and some common Florida bat species including the Seminole bat (*Lasiurus seminolus*) and northern yellow bat (*L. intermedius*) were not included in the program's identifiers. Given these shortcomings, species diversity may be understimated. Also, results for presence/absence of *L. borealis* are uncertain as this species' call is often confounded with *L. seminolus*.

Calls were segregated into nightly bins, and Jost diversity was calculated based on the Shannon-Wiener Diversity Index (Jost, 2006). Multiple regression and logistic models were developed in R (R Development Core Team, 2014) to test relationships between forest structure and landscape level parameters and six different response variables: overall abundance, diversity, and evening bat (*Nycticeus humeralis),* tricolored bat *(Perimyotis subflavus),* southeastern myotis *(Myotis austroriparius),* and big brown bat (*Eptesicus fuscus)* presence (Table 2). The four bats included in the regression models were selected because they were present in approximately equal numbers and should represent differing foraging strategies based on morphology. Model parameters were selected based on previous literature and relevance to management strategy. To improve model assumptions, parameters for community diversity models were normalized and diversity was log transformed, therefore changing Jost diversity into the Shannon-Weiner Diversity Index. For total site usage models, negative binomial generalized linear models were used. In all cases, the most informative models were selected based AICc (Akaike's Information Criterion for small sample sizes) value and AICc weight (Burnham and Anderson, 2002). AICc and AICc weight were calculated using R package AICmodavg (Mazerolle, 2015).

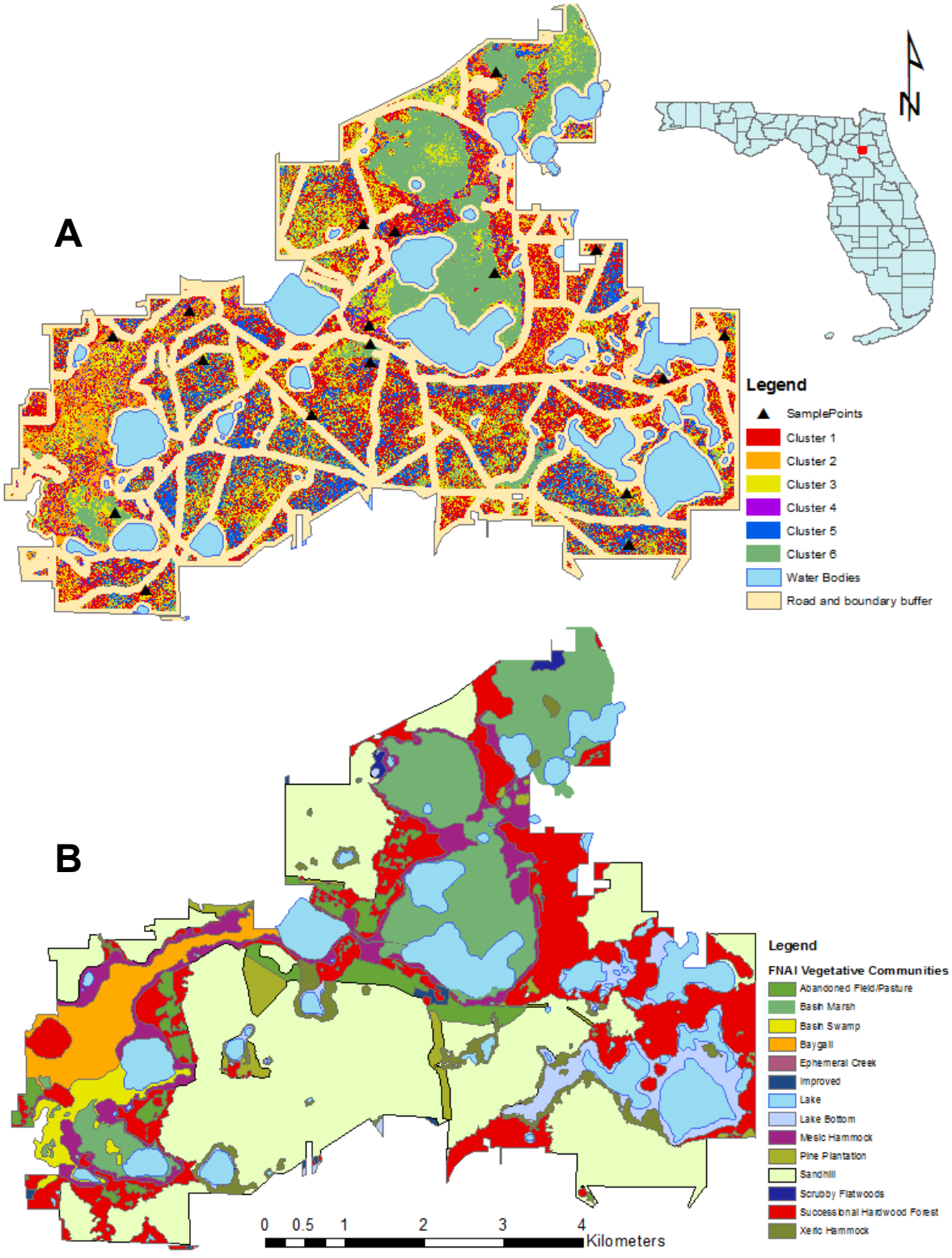

Figure 3: A) OSBS 5 x 5 m k-means cluster results; B) vegetative communities at OSBS as defined by Florida Natural Areas Inventory (FNAI)

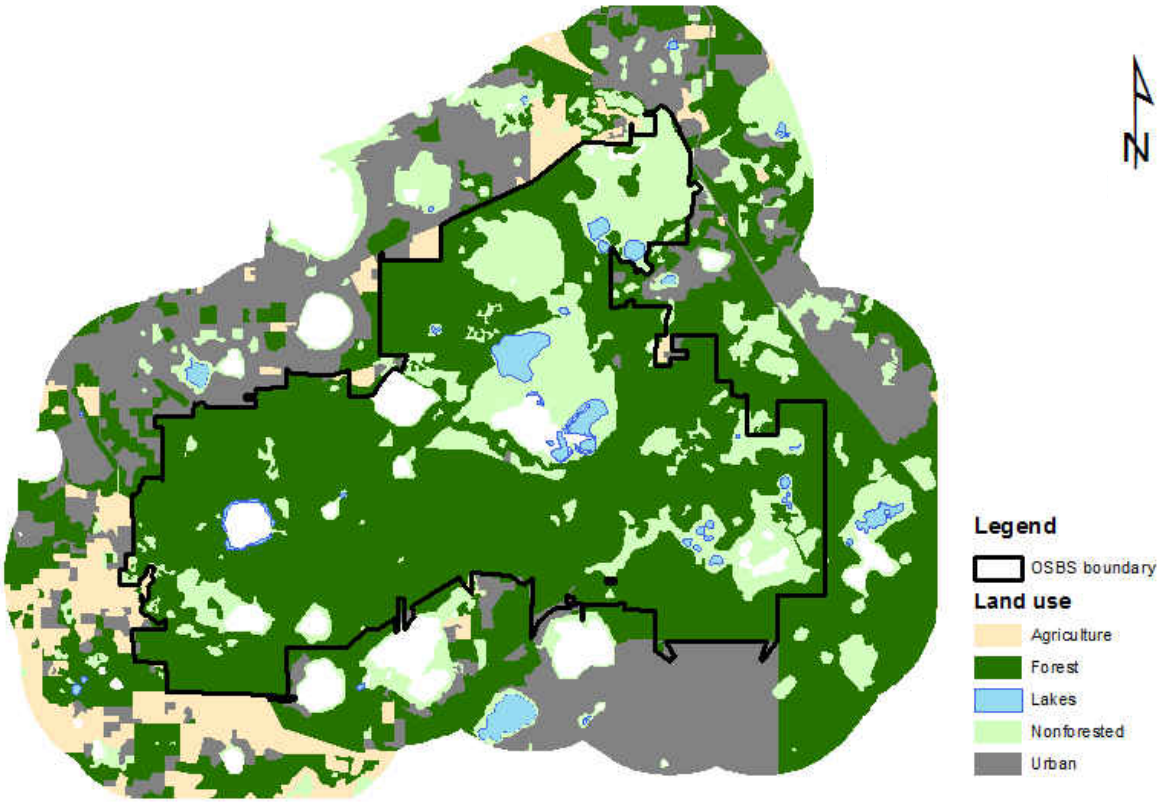

Figure 4: Level 1 FLUCCS designations for 1.5 km buffer around OSBS

Table 1: Final parameters used in models selection and their ecological significance

Parameter (abbreviation)	Ecological Significance
	Stand Level
Mean canopy height (CanMean)	Mean canopy height for each 5x5 m site (in m)
Rugosity (Rugosity)	Roughness of the outer canopy surface for each 5x5 m site measured by calculating the standard deviation of maximum canopy height
Proportion of returns (0-1.5 m (Prop015), 1.5-6 m. (Prop156), 6-12 (Prop612), 12 m and above (PropAb12))	The proportion of LiDAR returns in different height bins (related to the amount of clutter within the forest)
Entropy (Entropy)	The Jost diversity of vertical LiDAR return distributions
	Landscape Level
Area of standing water (AreaWater)	Area (in ha) of standing water (lakes, ponds) within 1.5 km buffer
Service road length (RoadLength)	Length (in m) of service roads in 1.5 km buffer (limited to areas within OSBS)
Proportion of urban land cover (PropUrban)	Proportion of 1.5 km buffer classified in FLUCCS as urban or utilities
Landscape heterogeneity (LandHeterogeneity)	The Jost diversity of k-means clusters within a 1.5 km buffer (limited to areas within OSBS)

Table 2: Parameters for numbered models.

Number	Parameters
1	CanopyMean+Entropy+Rugosity+Prop015+Prop156+Prop612
2	CanopyMean*Entropy+Rugosity+Prop015+Prop156+Prop612
3	CanopyMean+Entropy+Rugosity
4	CanopyMean*Entropy+Rugosity
5	CanopyMean+Entropy+Rugosity+Prop015+Prop156+Prop612+LandHeterogeneity
6	CanopyMean*Entropy+Rugosity+Prop015+Prop156+Prop612+LandHeterogeneity
7	CanopyMean+Entropy+Rugosity+Prop015+Prop156+Prop612+PropUrban+PercentWater+RoadLength+LandHeterogeneity
8	CanopyMean+Entropy+Rugosity+Prop015+Prop156+Prop612+PropUrban*LandHeterogeneity +PercentWater+RoadLength
9	CanopyMean+Entropy+Rugosity+Prop015+Prop156+Prop612+PropUrban+PercentWater*LandHeterogeneity +RoadLength
10	CanopyMean+Entropy+Rugosity+Prop015+Prop156+Prop612+PropUrban+PercentWater +RoadLength*LandHeterogeneity

RESULTS

K Means Clustering

The k-means cluster analysis defined vegetative structure at the 25 m^2 scale. Large basin marsh areas, which lacked canopy (cluster 6), were very homogenous throughout and closely correspond with the vegetation mapped by the Florida Natural Areas Inventory (FNAI) (Figure 3B). The finer scale of the k-means clustering allowed me to examine subtle differences in forest structure within larger vegetative communities. While the clusters do not exactly correspond to vegetative types, cluster 1 is more prominent within successional hardwood forest, cluster 2 is common throughout baygall, and cluster 5 is found throughout pine sandhills. Figure 5 shows boxplots of the canopy height (A) and rugosity (B) for each of the three sites chosen for each cluster.

LiDAR point cloud images (Figure 6) also reveal differences in forest structure. Each point cloud in Figure 66 represents a site within one of the six different k-means clusters. Main differences occur in overall canopy height, rugosity, and midstory clutter. For instance, cluster 1 had an open canopy with herbaceous ground cover. Clusters 2, 3, 4, and 5 had more closed canopies. The sites in cluster 6 were all comprised of basin marshes with different grass species as dominant vegetation. No tree or shrub canopy was present in this cluster. The representative site for cluster 2 had a higher rugosity than that for cluster 3 which had a more homogenous canopy height. The site shown for cluster 4 has less midstory clutter present, especially towards the left side of the image where an opening in vegetation can be seen.

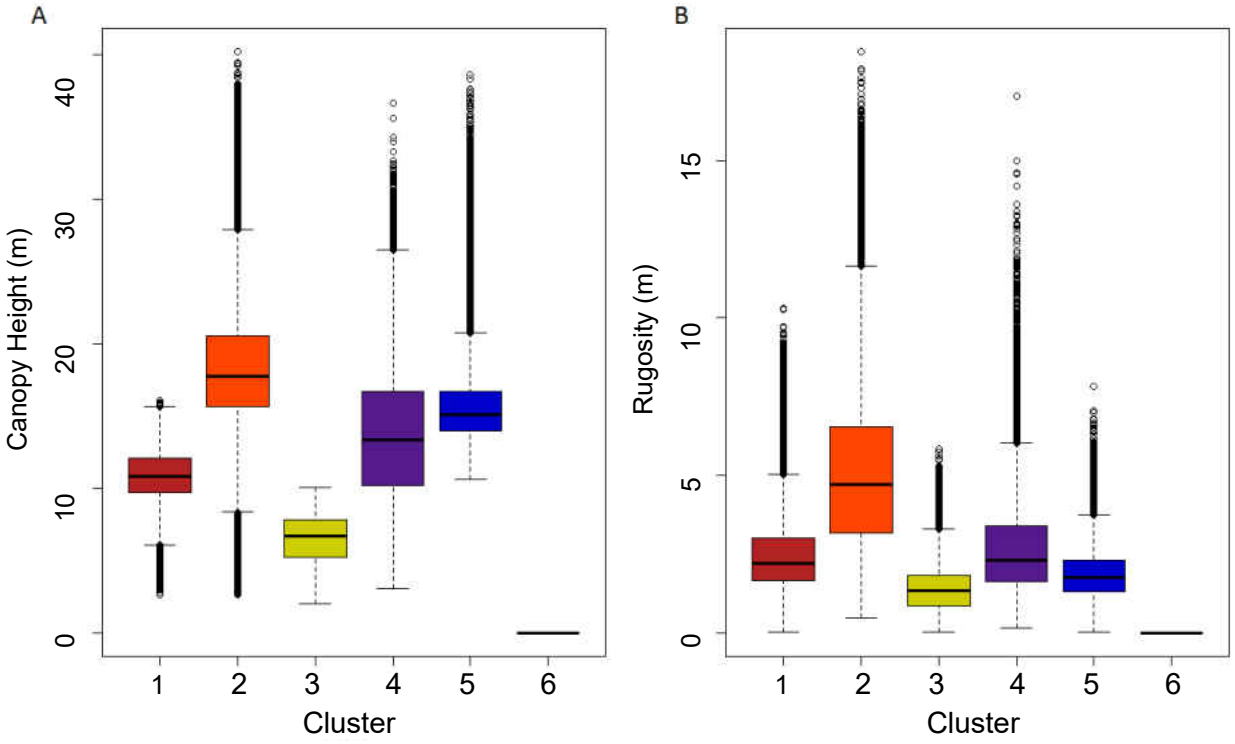

Figure 5: Cluster metrics for A) canopy mean and B) rugosity. Colors correspond to clusters from Figure 3A. The line within the boxplot is the median while the circles are outliers outside of one standard deviation from the mean.

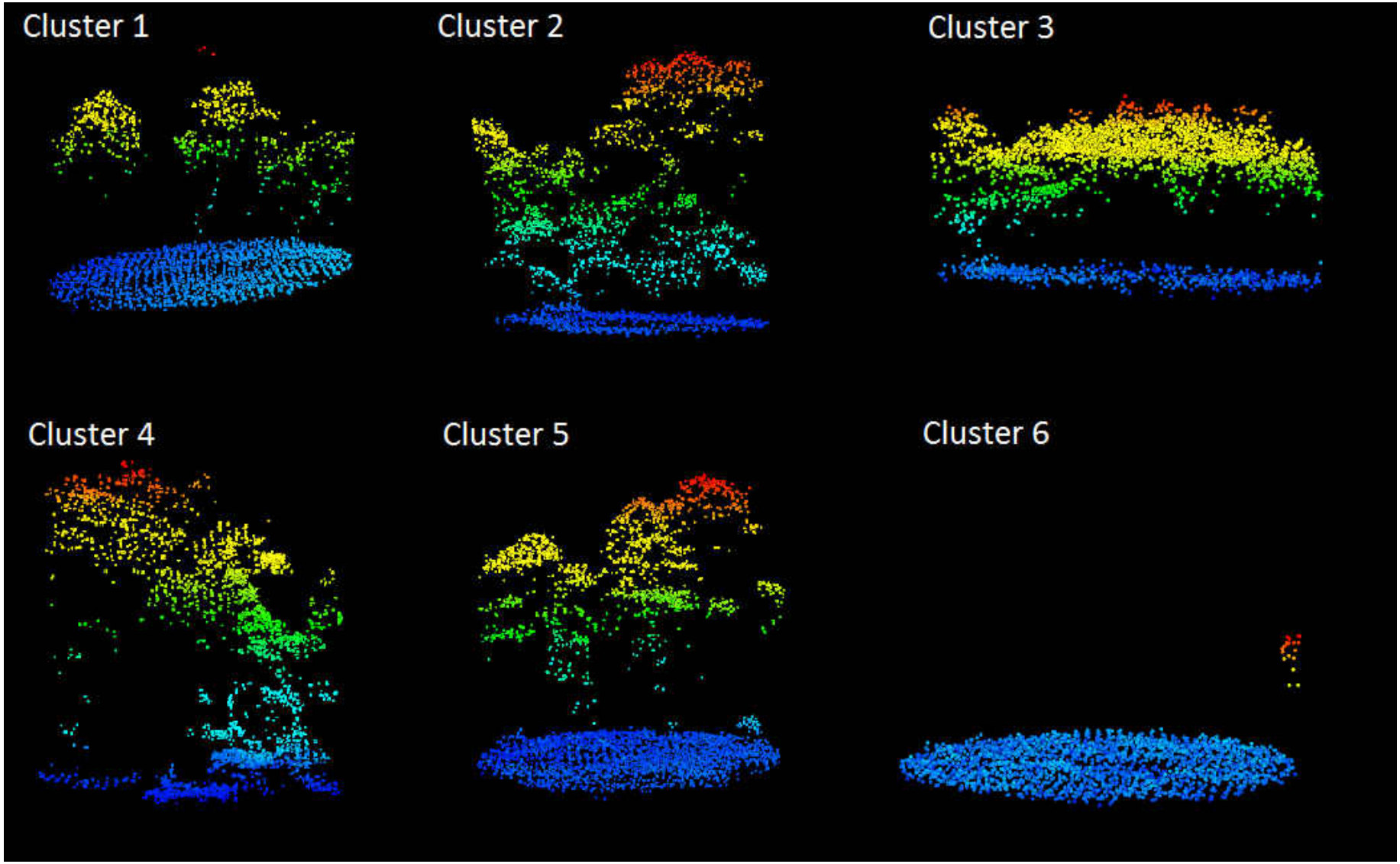

Figure 6: LiDAR point clouds for representative sites at each cluster; the radius of the ground surface (blue disk) is 12.5 m.

Acoustics Summary

Over 47 sample nights, a total of 27,481 bats calls were identified using Echoclass v. 3.1. There were 263 big brown bats, 16,533 eastern red bats, 696 hoary bats, 140 southeastern myotis, 344 evening bats, and 1,114 tricolored bats. Echoclass v. 3.1 also identified 373 silver-haired bats (*Lasionycteris noctivagans*), but these bats are not known to occur within Ordway-Swisher and so were very likely misidentified. These bats were still included in diversity calculations as they likely represented a species that was not included within the filter set. Figure 7 shows the total bat abundance at each site and Figure 8 shows the bat diversity for each site. Figure 9 shows the species accumulation curves for each cluster type. Most clusters approached an asymptote though not all species were detected in all clusters.

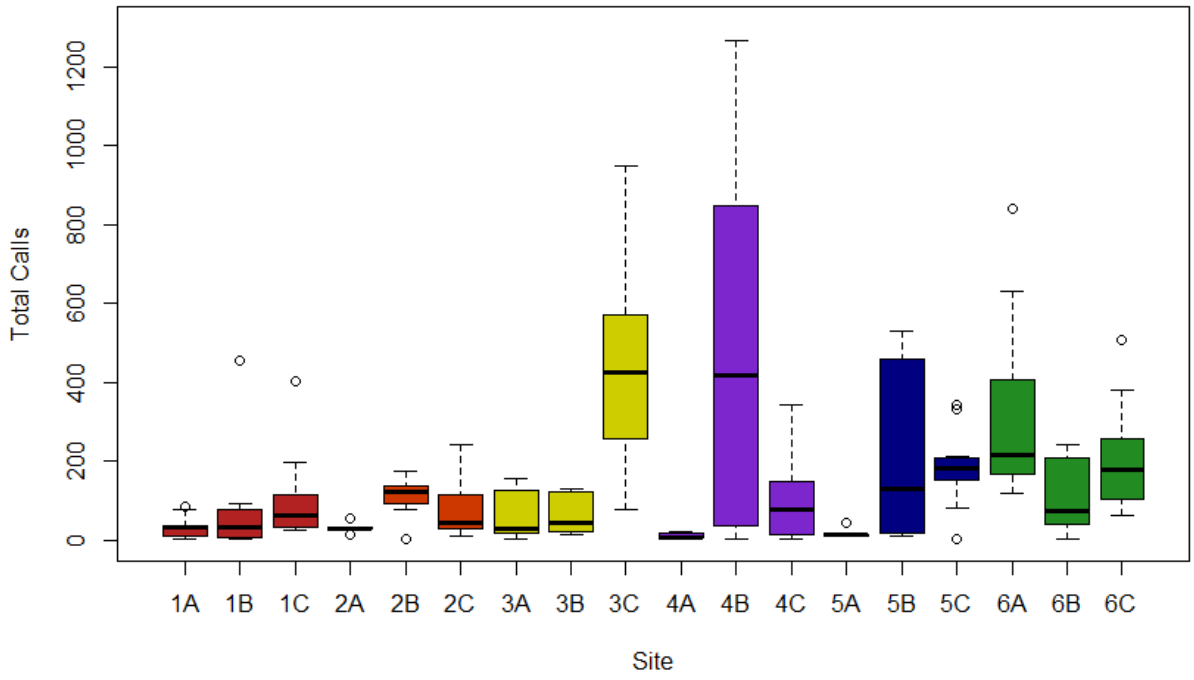

Figure 7: Total bat abundance by site; sites are color coded by cluster corresponding with Figure 3A. The line through the boxes represents the median while open circles are outlier points.

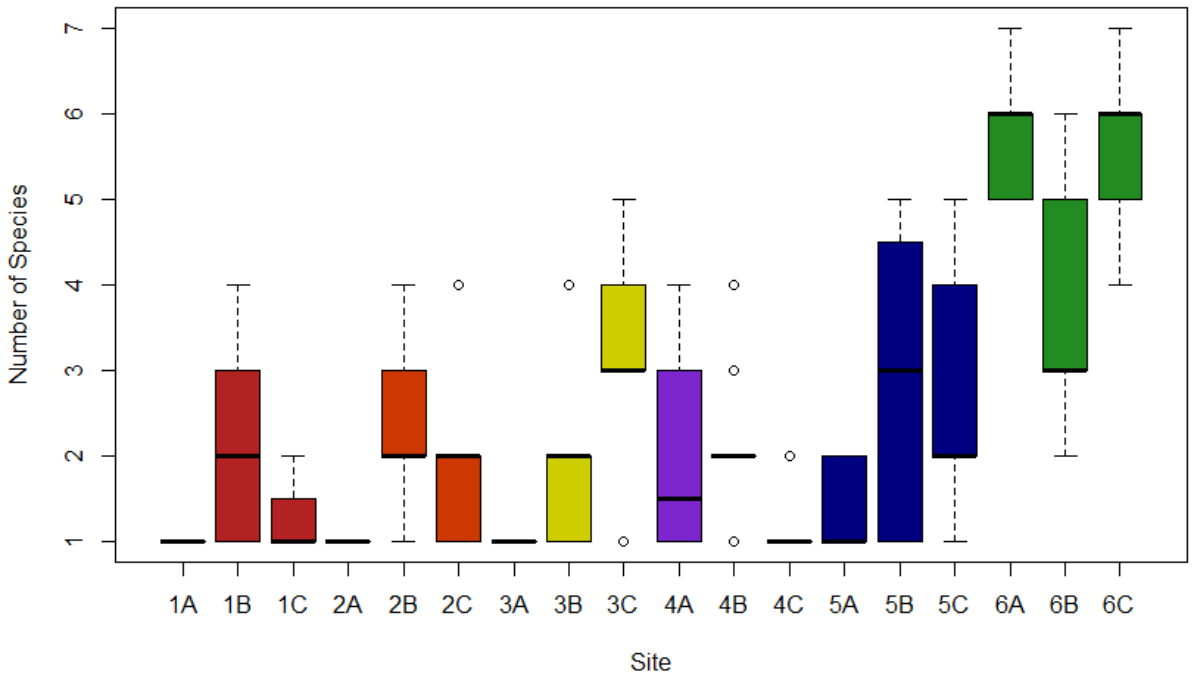

Figure 8: Jost bat diversity for each site; colors correspond to the clusters from Figure 3A. The line through the boxes represents the median while open circles are outlier points.

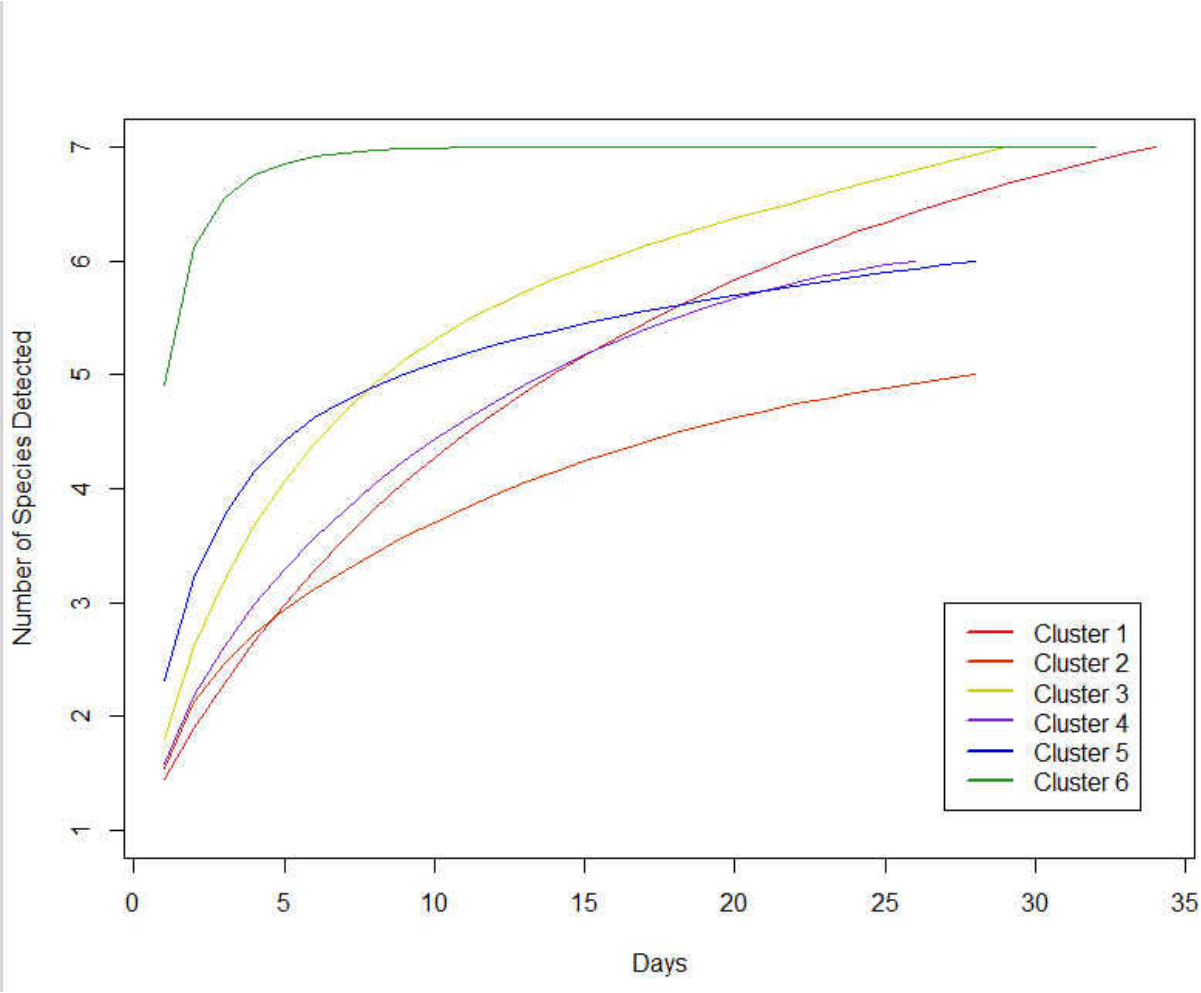

Figure 9: Species accumulation curves per cluster which are represented by different colored lines based on Figure 3A. EchoClass v 3.1 had the ability to identify 7 total species.

Model Selection

Overall Abundance Models

Because of close AIC weights and ΔAIC, it was not possible to pinpoint a single most informative overall abundance model (Appendix D, Table D1). Model 8 had an AIC of 1922.6, ΔAIC of -0.7, and AIC weight of 0.42. Model 9 had an AIC of 1923.7, ΔAIC of -0.9, and AIC weight of 0.30. Model 10 had an AIC of 1923.3, ΔAIC of -13.8, and AIC weight of 0.27. In all three models, proportion of binned returns (0-1.5 m, 1.5- 6 m, and 6-12 m) as well as length of service roads were negatively correlated with bat abundance. Models 9 and 10 also had a negative correlation between site usage and area of water. All of the models included mean canopy height, entropy, binned proportion of returns (0-1.5 m, 1.5-6 m, 6-12 m), proportion of urban lands, landscape heterogeneity, area of water, and length of service roads. Model 9 also included the interaction of landscape heterogeneity and the proportion of urban lands while model 10 included the interaction of landscape heterogeneity and water area. Model 8 had no interactive terms. Tables 3, 4, and 5 show the complete results for the three most informative abundance models.

Table 3: Results for most informative total abundance model.

	Estimate	Std. Error	z value	Pr(>|z|)
Intercept	13.66	2.630	5.195	<0.001
Mean canopy height	-0.0718	0.0477	-1.504	0.1325
Entropy	0.0561	0.2912	0.192	0.8474
Rugosity	-0.0320	0.2280	-0.141	0.888
Proportion of returns (0-1.5 m)	-3.240	1.021	-3.173	<0.01
Proportion of returns (1.5-6 m)	-16.34	6.830	-2.393	<0.05
Proportion of returns (6-12 m)	-4.415	1.142	-3.864	<0.001
Proportion of urban lands	-7.656	1.385	-5.527	<0.001
Water Area	-0.0106	0.0029	-3.616	<0.001
Length of service roads	-0.0001	-0.00005	-2.258	<0.05
Landscape heterogeneity	-0.4294	0.4651	-0.923	0.356

Table 4: Results for second most informative total abundance model.

	Estimate	Std. Error	z value	Pr(>|z|)
Intercept	14.78	2.714	5.445	<0.001
Mean canopy height	-0.0797	0.0487	-1.639	0.101
Entropy	0.0650	0.2938	0.221	0.825
Proportion of returns (0-1.5 m)	-2.629	1.132	-2.322	<0.05
Proportion of returns (1.5-6 m)	-19.50	8.050	-2.422	<0.05
Proportion of returns (6-12 m)	-3.793	1.233	-3.075	<0.01
Proportion of urban lands	-31.93	19.68	-1.622	0.105
Landscape heterogeneity	-0.7683	0.5057	-1.519	0.129
Water area	-0.0096	0.0030	-3.160	<0.01
Length of service roads	-0.0001	-0.00005	-2.356	<0.05
ProportionUrban:LandscapeHetereogeneity	5.439	4.348	1.251	0.211

Table 5: Results for third most informative total abundance model.

	Estimate	Std. Error	z value	Pr(>|z|)
Intercept	8.951	4.399	2.035	<0.05
Mean canopy height	-0.0758	0.0487	-1.557	0.120
Entropy	0.1245	0.2952	0.422	0.673
Rugosity	-0.1019	0.2358	-0.432	0.666
Proportion of returns (0-1.5 m)	-3.215	1.029	-3.125	<0.01
Proportion of returns (1.5-6 m)	-16.94	6.891	-2.458	<0.05
Proportion of returns (6-12 m)	-4.337	1.140	-3.805	<0.001
Proportion of urban lands	-7.439	1.421	-5.236	<0.001
Landscape heterogeneity	0.6202	0.9123	0.680	0.497
Water area	0.0622	0.0637	0.978	0.328
Length of service roads	-0.0001	0.00005	-2.359	<0.05
LandscapeHeterogeneity:WaterArea	-0.0161	0.0141	-1.144	0.252

Bat Community Diversity Models

Model 10 which included mean canopy height, entropy, rugosity, area of water, proportion of binned returns (0-1.5 m, 1.5-6 m, 6-12 m.), proportion of urban land, service road length, and landscape heterogeneity within buffer space as well as the interactions between several of these parameters was the most informative model with an adjusted R^2 of 0.68, relative AICc weight of 1.0 and ΔAIC of -21.99 (Appendix D, Table D2). Mean canopy height, binned proportion of returns (0-1.5 m, 1.5 – 6 m, and 6-12 m), area of water, road length, and landscape heterogeneity all had significant negative relationships to bat community diversity whereas entropy and the interaction of road length and landscape heterogeneity both had a positive relationship to bat community diversity. Rugosity and proportion of urban lands within the 1.5 km buffer did not have significant relationships to bat community diversity. Table 6 shows the coefficients and p-values of parameters for the most parsimonious model.

Table 6: Results for most informative community diversity model.

	Estimate	Std. Error	t value	Pr(>|t|)
Intercept	0.209	0.021	9.949	<0.001
Canopy mean	-0.069	0.010	-6.715	<0.001
Entropy	0.176	0.059	2.995	<0.01
Rugosity	-0.005	0.046	-0.118	0.906
Proportion of returns (0-1.5 m)	-1.036	0.204	-5.083	<0.001
Proportion of returns (1.5-6 m)	-3.723	1.397	-2.665	<0.01
Proportion of returns (6-12 m)	-1.739	0.229	-7.613	<0.001
Proportion of urban lands	-0.173	0.275	-0.628	0.531
Area of Water	-0.0016	0.0006	-2.610	<0.01
Service road length	-0.00003	0.000009	-3.159	<0.01
Landscape heterogeneity	-0.280	0.094	-2.985	<0.01
RoadLength:LandscapeHeterogeneity	0.0001	0.00001	7.857	<0.001

Logistic Regression Models for Evening Bat (N. humeralis)

Model 6 which included mean canopy height, entropy, rugosity, proportion of binned returns (0-1.5 m, 1.5-6 m, 6-12 m), landscape heterogeneity and the interaction between mean canopy height and entropy was the most informative logistic model for *N. humeralis* with an AICc of 136.71, AICc weight of 0.98, and ΔAICc of -9.11 (Appendix D, Table D3). Mean canopy height and entropy were both negatively related to *N. humeralis* detection while the interaction of mean canopy height and entropy was positively related to detection of *N. humeralis*. (Table 7).

Table 7: Results for most informative logistic model, evening bat (*N. humeralis*).

	Estimate	Std. Error	z value	Pr(>|z|)
(Intercept)	38.70	14.15	2.734	<0.01
Mean canopy height	-1.865	0.708	-2.633	<0.01
Entropy	-8.991	3.074	-2.924	<0.01
Rugosity	0.029	0.774	0.037	0.970
Proportion of returns (0 – 1.5 m)	-0.116	4.311	-0.027	0.979
Proportion of returns (1.5 – 6 m)	-90.00	56.98	-1.580	0.114
Proportion of returns (6 – 12 m)	-1.667	4.371	-0.381	0.703
Landscape heterogeneity	-5.214	2.085	-2.500	0.012
MeanCanopyHeight:Entropy	0.997	0.379	2.632	<0.01

Logistic Regression Models for Tricolored bat (P. subflavus)

Model 10 was the most informative model for presence of *P. subflavus* with an AICc of 185.63, AICc weight of 0.84, and ΔAIC of 4.88 (Appendix D, Table D4). Model parameters were mean canopy height, entropy, rugosity, binned proportion of returns (0-1.5 m, 1.5-6 m, 6-12 m), proportion of urban lands, area of water, length of roads, landscape heterogeneity, and the interaction of road length and landscape heterogeneity. Area of water and the interaction between road length and landscape heterogeneity were positively related to *P. subflavus* presence while the proportion of returns from 6-12

m, length of service roads, and landscape heterogeneity were negatively related to *P. subflavus* presence (Table 8).

Table 8: Results for most informative logistic model, tricolored bat (*P. subflavus*).

	Estimate	Std. Error	z value	Pr(>|z|)
(Intercept)	45.890	14.10	3.254	<0.01
Mean canopy height	-0.037	0.138	-0.270	0.787
Entropy	-1.087	1.053	-1.032	0.302
Rugosity	-0.110	0.543	-0.203	0.839
Proportion of returns (0 – 1.5m)	-1.373	2.946	-0.466	0.641
Proportion of returns (1.5 – 6 m)	13.187	16.33	0.807	0.419
Proportion of returns (6 – 12 m)	-7.709	3.731	-2.066	<0.05
Proportion of urban lands	-7.018	3.892	-1.803	0.071
Water area	0.015	0.007	2.004	<0.05
Service road length	-0.003	0.001	-2.435	<0.05
Landscape heterogeneity	-9.928	3.532	-2.811	<0.01
ServiceRoadLength:LandscapeHeterogeneity	0.0006	0.0003	2.422	<0.05

Logistic Regression Models for Southeastern Myotis (M. austroriparius)

Model 5 was the most informative model of the logistic regression models for the southeastern myotis (Appendix D, Table D5). It had an AICc of 130.65, a ΔAIC of -2.14, and an AICc weight of 0.50. Model parameters for model 5 were mean canopy height, entropy, rugosity, binned proportion of returns (0-1.5 m, 1.5-6 m, 6-12 m), and landscape heterogeneity. Of these, entropy had a positive relationship with southeastern myotis presence while proportion of returns from 6-12 m and landscape heterogeneity had negative relationships with the presence of this species (Table 9).

Table 9: Results for most informative logistic model, southeastern myotis (*M. austroriparius*).

	Estimate	Std. Error	z value	Pr(>|z|)
Intercept	12.04	6.108	1.971	<0.05
Mean canopy height	-0.219	0.131	-1.671	0.095
Entropy	2.240	0.815	2.749	<0.01
Rugosity	-0.716	0.663	-1.080	0.280
Proportion of returns (0-1.5 m)	-4.926	2.832	-1.740	0.082
Proportion of returns (1.5-6 m)	-5.447	27.47	-0.198	0.843
Proportion of returns (6-12 m)	-17.10	4.753	-3.596	<0.001
Landscape heterogeneity	-2.066	0.837	-2.468	<0.05

Logistic Regression Models for Big Brown Bat (E. fuscus)

Three logistic models had comparable AICc weights for the big brown bat (Appendix D, Table D6). These were models 7 (AICc of 91.46, ΔAICc of -0.08, AICc weight of 0.33, Table 10), 10 (AICc of 91.54, ΔAICc of -0.64, AICc weight of 0.32, Appendix D, Table D7), and 9 (AICc of 92.10, ΔAICc of -2.19, AICc weight of 0.24, Appendix D, Table D8). All three models included mean canopy height, entropy, rugosity, binned proportion of returns (0-1.5 m, 1.5-6 m, 6-12 m), landscape heterogeneity, proportion of urban lands, area of water, and length of service roads. Model 10 included the interaction between length of service roads and landscape heterogeneity while model 9 included the interaction of landscape heterogeneity and area of water. Model 7 had no interactive terms. In all three models, entropy had a positive relationship to presence of the big brown bat while proportion of returns between 0-1.5 m

and 6-12 m had a negative relationship to the presence of this species. Two of the models (7 and 9) also showed a negative relationship between the length of service roads and presence of this species.

Table 10: Results for most informative logistic model, big brown bat (*E. fuscus*).

	Estimate	Std. Error	z value	Pr(>|z|)
Intercept	44.64	16.56	2.696	<0.01
Mean canopy height	-0.6004	0.2508	-2.394	<0.05
Entropy	3.733	1.592	2.344	<0.05
Rugosity	-4.782	3.476	-1.376	0.169
Proportion of returns (0-1.5 m)	-19.79	8.195	-2.415	<0.05
Proportion of returns (1.5-6 m)	17.44	59.57	0.293	0.770
Proportion of returns (6-12 m)	-26.67	9.397	-2.838	<0.01
Proportion of urban lands	-2.432	6.100	-0.399	0.690
Area of water	-0.0421	0.0270	-1.565	0.118
Length of service roads	-0.0004	-0.0002	-2.762	<0.01
Landscape heterogeneity	-3.211	1.649	-1.948	0.051

DISCUSSION

Increasing the proportion of returns in any single bin (0-1.5 m, 1.5-6 m, 6-12 m) had a negative effect on overall usage of sites by bats. This may be due to lowered detectability in cluttered environments, though Patriquin and Barclay (2003) showed that structural clutter does not affect detection rates of bats calling at the 40 Hz range. More likely is that the majority of bats were detected within the unforested basin marsh sites which had few aboveground returns. Though insect abundance was perceived to be higher in these areas, it is likely that bats were preferentially foraging in these sites to minimize difficulties associated with tracking prey while simultaneously avoiding obstacles within their flight paths (Simmons, Fenton and O'Farrell, 1979). Within South Carolina, wetlands were also shown to be important foraging habitat for bats (Menzel, Menzel, Kilgo *et al.*, 2005a), so it is likely that bats within Florida also preferentially forage in similar wetland habitats such as basin marsh.

Several parameters had strong correlations with bat community diversity. Maximizing the vertical foliage height diversity (entropy) positively related to bat community diversity, following the same patterns of bird species diversity (Goetz *et al.*, 2007, MacArthur and MacArthur, 1961). By the same token, increases in vegetative clutter throughout the midstory corresponded to lower levels of bat community diversity. This is likely because those species which are morphologically clutter intolerant would be unable to forage within highly cluttered spaces (Brigham, Grindal, Firman *et al.*, 1997, Ford, Menzel, Rodrigue *et al.*, 2005, Marciente, Brobrowiec and Magnusson, 2015, Rainho, Augusto and Palmeirim, 2010, Sleep and Brigham, 2003). It is surprising that the length of service roads within the buffer space surrounding plots negatively relates to bat species diversity when it well known that many bats use roads and forest edge as flyways and foraging area (Grindal and Brigham, 1999, Hein, Castleberry and Miller, 2009). However, other studies (Bender, Castleberry, Miller *et al.*, 2015, Loeb and O'Keefe, 2006) show little support for roads as a feature promoting bat occupancy, especially at the landscape scale. The relationship between roads and bat diversity within forested areas may also be better captured by measuring distance to roads instead of overall length of roads within a study area (Rainho and

Palmeirim, 2011). It is possible that the roads may have been important edge habitat for the bats in this study, however since roads were not directly compared to natural spaces, the results may be conflated.

Landscape heterogeneity, measured as the Jost diversity of k-means cluster results within the 1.5 km buffer surrounding each sample point, also had a negative relationship to bat community diversity. One reason for this may be that having to navigate through a large variety of differing forest types would make commuting to foraging spaces more difficult for bats that specialize in open area flight. Because the landscape heterogeneity measure was taken at a very fine scale (5 x 5 m), it is possible that this may not have captured a scale relevant to the long-range species present within OSBS (Stephens, Koons, Rotella *et al.*, 2003).

Area of water was also had a negative relationship to bat community diversity, though most of the species present within OSBS are known to forage over water. This may be in part because the water bodies considered were permanent lakes and ponds that were measured using GIS layers. Ephemeral sources of water, such as temporarily inundated swampy areas which may be important sources of drinking water and foraging habitat for clutter-adapted species such as the tricolored bat, were not mapped or considered as part of this study. Bender *et al.* (2015) found a negative relationship between site occupancy of tricolored bats (*P. subflavus*) and distance to water. They used similar methods to map water sources and likewise neglected ephemeral water sources. Their findings are similar to ours for bat diversity, but opposite for the presence of tricolored bats which indicates that perhaps the tricolored bats found at our study site were not particularly dependent on ephemeral sources of water.

Vertical foliage height diversity was positively related to presence of southeastern myotis and big brown bats and negatively related to presence of evening bats. Because the big brown bat is a habitat generalist that forages both in stand interiors and edges (Brigham, 1991), increases in foliage height diversity may have created more foraging space for this species to use. Negative relationships between presence of big brown bat and evening bat to canopy height may be related to these species being over canopy flyers (Menzel, Menzel, Kilgo *et al.*, 2005b). Bats flying over lower canopies may have been detected whereas those flying over tall canopies remained undetected.

LiDAR-derived forest structure parameters added predictive power to models of bat species diversity, occurrence, and site utilization. LiDAR allows land managers to quickly and effectively categorize forest structure over an entire landscape so they can make more informed decisions on where to focus management efforts (Merrick *et al.*, 2012). LiDAR not only allows managers to inventory forests and determine structural parameters such as height and entropy at fine scales, it also can be useful in determining successional stages of fire-managed communities (Angelo, Duncan and Weishampel, 2010) at scales relevant to species conservation and management. Using fire to manage ecosystems is critically important in the southeastern coastal plain of the United States, and though not considered in this study, is expected to have an effect on bat species living within fire managed areas (Armitage and Ober, 2012) since fire changes vegetation structure by thinning overgrown stands and allowing grasses and herbaceous ground vegetation to prosper. Alternatively, stands of pine savanna which are fire suppressed suffer from hardwood encroachment and increased midstory clutter.

The use of LiDAR has led to advances in the understanding of species/habitat relationships because LiDAR measurements can tease out nuanced patterns from very fine (tree branch) to coarse (landscape-level) scales (Davies and Asner, 2014). LiDAR is also useful in creating indices of structural diversity over large landscapes (Listopad, Masters, Drake *et al.*, 2015) which allows researchers to broaden their understanding of multiple indicators of biodiversity (Noss, 1990) by coupling monitoring biodiversity at the species level with understanding of landscape structure and disturbance regimes. Taking LiDAR inventories of managed sites could prove useful to managers who must make decisions on how to best conserve plant and animal species at differing scales.

Given the continental scale LiDAR collection done by NEON, it is will be possible to extend this and similar studies throughout the United States allowing researchers to understand large scale patterns of bat diversity and habitat use. These studies could be conducted regularly to monitor changes in both habitat and species composition throughout the contiguous United States. Though all of the species present within this area of Florida are common, other studies have shown benefits to monitoring common species (Agosta, 2002), including detecting possible declines of these species (Winhold, Kurta and Foster,

2008). These studies could be supported by citizen scientists as acoustic data collection does not require strict permitting. However, since acoustic studies can only provide researchers with information about habitat use (Miller, Arnett and Lacki, 2003), further research using different methods would be advised in order to determine habitat preference.

Future studies could also expand this research by including multiple detector levels to better understand relationships between structural parameters and above canopy flyers (Menzel *et al.*, 2005b). This study could also be improved by considering measures at the stand level in addition to site and landscape level parameters, as all three levels have been shown to affect bat presence (Loeb and O'Keefe, 2006). LiDAR-derived parameters such as landscape heterogeneity may be more meaningful at the stand level instead of the landscape level.

The conservation of bat species is becoming increasingly important as bats face anthropogenic-related pressures including disease (Frick *et al.*, 2010), wind turbine mortality (Arnett *et al.*, 2008), and habitat destruction and degradation. Even common bat species such as the eastern red bad may be in decline (Winhold *et al.*, 2008), and as important habitat such as pine savannas are increasingly converted into agricultural and urban lands (Wear and Greis, 2002) more species are expected to be affected. In order to preserve a high diversity of bat species, it is integral to understand their relationships with complex environments. LiDAR is an excellent tool to help researchers understand species/habitat dynamics over large scales.

APPENDIX A: CORRELATION MATRICES

Table A1: Correlation matrix of LiDAR parameters for k-means clustering (extends through page 65); blue cells are positively related and red cells are negatively related. ND values represent no data.

	TotalReturns	ElevMin	ElevMax	ElevMean	ElevMode
TotalReturns	1.0000	-0.1753	0.6304	0.4975	0.4686
ElevMin	-0.1753	1.0000	0.1237	0.4227	0.3911
ElevMax	0.6304	0.1237	1.0000	0.8592	0.7233
ElevMean	0.4975	0.4227	0.8592	1.0000	0.8969
ElevMode	0.4686	0.3911	0.7233	0.8969	1.0000
ElevStdDev	0.5365	-0.2582	0.7641	0.4781	0.3863
ElevVar	0.5365	-0.2582	0.7641	0.4781	0.3863
ElevCV	0.2714	-0.5784	0.2711	-0.1388	-0.1916
ElevIQ	0.4580	-0.2566	0.6096	0.3254	0.2370
ElevSkew	-0.2518	-0.2778	-0.3672	-0.6453	-0.6858
ElevKurtosis	0.2111	0.1792	0.2113	0.3412	0.3618
ElevAAD	0.5071	-0.2670	0.7115	0.4182	0.3290
ElevL1	0.4975	0.4227	0.8592	1.0000	0.8969
ElevL2	0.5211	-0.2577	0.7364	0.4435	0.3536
ElevL3	-0.2614	-0.1568	-0.3796	-0.6023	-0.6901
ElevL4	0.3148	0.1068	0.4228	0.4308	0.4502
ElevLCV	0.2482	-0.5686	0.2377	-0.1719	-0.2234
ElevLSkewness	-0.2345	-0.2156	-0.3474	-0.5888	-0.6634
ElevLKurtosis	0.0825	0.2136	0.1187	0.2518	0.2886
ElevP01	0.0553	0.8811	0.3273	0.6296	0.5846
ElevP05	0.2168	0.7530	0.4797	0.7745	0.7159
ElevP10	0.2893	0.6791	0.5583	0.8437	0.7864
ElevP20	0.3742	0.5794	0.6625	0.9185	0.8624
ElevP25	0.4006	0.5434	0.6985	0.9401	0.8860
ElevP30	0.4251	0.5093	0.7316	0.9570	0.9012
ElevP40	0.4634	0.4525	0.7869	0.9786	0.9164
ElevP50	0.4879	0.4016	0.8314	0.9871	0.9107
ElevP60	0.5092	0.3569	0.8672	0.9846	0.8922
ElevP70	0.5296	0.3121	0.8999	0.9735	0.8644
ElevP75	0.5403	0.2901	0.9153	0.9648	0.8477
ElevP80	0.5486	0.2671	0.9302	0.9534	0.8281
ElevP90	0.5749	0.2166	0.9624	0.9241	0.7871
ElevP95	0.5879	0.1824	0.9798	0.8997	0.7597
ElevP99	0.6118	0.1429	0.9953	0.8712	0.7321
Return1Above3	0.9999	-0.1708	0.6198	0.4929	0.4658
Return2Above3	0.8527	-0.2406	0.6575	0.4273	0.3901
Return3Above3	0.0416	0.0032	0.0561	0.0488	0.0421
Return4Above3	ND	ND	ND	ND	ND
Return5Above3	ND	ND	ND	ND	ND
Return6Above3	ND	ND	ND	ND	ND
Return7Above3	ND	ND	ND	ND	ND
Return8Above3	ND	ND	ND	ND	ND
Return9Above3	ND	ND	ND	ND	ND
OtherReturnAbove3	ND	ND	ND	ND	ND
PercentFirstAbove3	0.9776	-0.1503	0.6997	0.5422	0.4999
PercentAllAbove3	0.9779	-0.1896	0.6875	0.5110	0.4709

	TotalReturns	ElevMin	ElevMax	ElevMean	ElevMode
AllDivFirstTimes100	0.9774	-0.1554	0.7075	0.5436	0.4989
FirstAbove3	0.9999	-0.1708	0.6198	0.4929	0.4658
AllAbove3	1.0000	-0.1753	0.6304	0.4975	0.4686
PercentAboveMean	0.8188	-0.1095	0.7149	0.6217	0.6026
PercentFirstAboveMode	0.6303	-0.1537	0.4952	0.3184	0.0896
PercentAllAboveMean	0.8247	-0.1422	0.7039	0.5951	0.5784
PercentAllAboveMode	0.6240	-0.1838	0.4755	0.2859	0.0568
AllAboveMeanDivByFirstTimes100	0.8198	-0.1126	0.7174	0.6201	0.5997
AllAboveModeDivByFirstTimes100	0.6283	-0.1559	0.4952	0.3152	0.0845
FirstAboveMean	0.9915	-0.1393	0.6499	0.5665	0.5555
FirstAboveMode	0.9720	-0.1904	0.4950	0.3376	0.1493
AllAboveMean	0.9916	-0.1418	0.6521	0.5655	0.5535
AllAboveMode	0.9717	-0.1926	0.4959	0.3350	0.1439
TotalFirst	-0.0807	-0.1134	0.0260	0.0193	0.0453
TotalAll	0.0294	-0.0701	0.0981	0.1023	0.1188
ElevMADMedian	0.4745	-0.2377	0.6143	0.3386	0.2509
ElevMADMode	0.3738	-0.2182	0.5244	0.2693	0.1413
CanopyReliefRatio	0.2416	0.3742	0.3837	0.6968	0.7192
ElevQuadraticMean	0.5171	0.3761	0.8911	0.9959	0.8839
ElevCubicMean	0.5317	0.3394	0.9143	0.9871	0.8681

	ElevStdDev	ElevVar	ElevCV	ElevIQ	ElevSkew	ElevKurtosis
TotalReturns	0.5365	0.5365	0.2714	0.4580	-0.2518	0.2111
ElevMin	-0.2582	-0.2582	-0.5784	-0.2566	-0.2778	0.1792
ElevMax	0.7641	0.7641	0.2711	0.6096	-0.3672	0.2113
ElevMean	0.4781	0.4781	-0.1388	0.3254	-0.6453	0.3412
ElevMode	0.3863	0.3863	-0.1916	0.2370	-0.6858	0.3618
ElevStdDev	1.0000	1.0000	0.7587	0.9030	-0.1562	-0.1361
ElevVar	1.0000	1.0000	0.7587	0.9030	-0.1562	-0.1361
ElevCV	0.7587	0.7587	1.0000	0.7879	0.3451	-0.4083
ElevIQ	0.9030	0.9030	0.7879	1.0000	0.0102	-0.4103
ElevSkew	-0.1562	-0.1562	0.3451	0.0102	1.0000	-0.4169
ElevKurtosis	-0.1361	-0.1361	-0.4083	-0.4103	-0.4169	1.0000
ElevAAD	0.9881	0.9881	0.7947	0.9502	-0.0873	-0.2473
ElevL1	0.4781	0.4781	-0.1388	0.3254	-0.6453	0.3412
ElevL2	0.9938	0.9938	0.7786	0.9360	-0.1100	-0.2063
ElevL3	-0.2910	-0.2909	0.1780	-0.1444	0.8949	-0.2412
ElevL4	0.2243	0.2243	-0.1084	-0.1002	-0.4124	0.7973
ElevLCV	0.7329	0.7329	0.9944	0.7971	0.3784	-0.4707
ElevLSkewness	-0.2308	-0.2308	0.2355	-0.0720	0.9519	-0.3002
ElevLKurtosis	-0.1956	-0.1956	-0.4446	-0.5095	-0.3609	0.8966
ElevP01	-0.1351	-0.1351	-0.5821	-0.1642	-0.4159	0.2931
ElevP05	-0.0211	-0.0211	-0.5575	-0.0993	-0.5489	0.4283
ElevP10	0.0615	0.0615	-0.5196	-0.0617	-0.6291	0.5005
ElevP20	0.2009	0.2009	-0.4181	0.0287	-0.7066	0.5261
ElevP25	0.2567	0.2567	-0.3685	0.0768	-0.7242	0.5062
ElevP30	0.3085	0.3085	-0.3184	0.1323	-0.7312	0.4762
ElevP40	0.4004	0.4004	-0.2233	0.2357	-0.7244	0.4026
ElevP50	0.4783	0.4783	-0.1367	0.3254	-0.6998	0.3300
ElevP60	0.5436	0.5436	-0.0606	0.4011	-0.6627	0.2691
ElevP70	0.6047	0.6047	0.0149	0.4723	-0.6128	0.2167
ElevP75	0.6339	0.6339	0.0530	0.5049	-0.5835	0.1971
ElevP80	0.6633	0.6633	0.0925	0.5313	-0.5505	0.1816
ElevP90	0.7177	0.7176	0.1723	0.5735	-0.4735	0.1767
ElevP95	0.7449	0.7449	0.2192	0.5936	-0.4231	0.1870
ElevP99	0.7615	0.7615	0.2592	0.6066	-0.3777	0.2043
Return1Above3	0.5201	0.5201	0.2568	0.4418	-0.2537	0.2215
Return2Above3	0.7569	0.7569	0.5283	0.6891	-0.1651	-0.0282
Return3Above3	0.0510	0.0510	0.0181	0.0429	-0.0165	-0.0019
Return4Above3	ND	ND	ND	ND	ND	ND
Return5Above3	ND	ND	ND	ND	ND	ND
Return6Above3	ND	ND	ND	ND	ND	ND
Return7Above3	ND	ND	ND	ND	ND	ND
Return8Above3	ND	ND	ND	ND	ND	ND
Return9Above3	ND	ND	ND	ND	ND	ND
OtherReturnAbove3	ND	ND	ND	ND	ND	ND
PercentFirstAbove3	0.6167	0.6167	0.3348	0.5398	-0.2409	0.1656
PercentAllAbove3	0.6331	0.6331	0.3755	0.5628	-0.2136	0.1402

	ElevStdDev	ElevVar	ElevCV	ElevIQ	ElevSkew	ElevKurtosis
AllDivFirstTimes100	0.6320	0.6320	0.3507	0.5556	-0.2368	0.1528
FirstAbove3	0.5201	0.5201	0.2568	0.4418	-0.2537	0.2215
AllAbove3	0.5365	0.5365	0.2714	0.4580	-0.2518	0.2111
PercentAboveMean	0.6241	0.6241	0.2668	0.5154	-0.4181	0.2089
PercentFirstAboveMode	0.4348	0.4348	0.3122	0.3953	-0.0229	0.1500
PercentAllAboveMean	0.6338	0.6338	0.2966	0.5309	-0.3950	0.1912
PercentAllAboveMode	0.4361	0.4361	0.3377	0.4024	0.0044	0.1330
AllAboveMeanDivByFirstTimes100	0.6289	0.6289	0.2734	0.5206	-0.4127	0.2048
AllAboveModeDivByFirstTimes100	0.4378	0.4378	0.3179	0.3993	-0.0173	0.1457
FirstAboveMean	0.5473	0.5473	0.2185	0.4464	-0.3935	0.2412
FirstAboveMode	0.4129	0.4129	0.2658	0.3570	-0.0761	0.1984
AllAboveMean	0.5513	0.5513	0.2237	0.4506	-0.3897	0.2383
AllAboveMode	0.4166	0.4166	0.2720	0.3618	-0.0705	0.1936
TotalFirst	0.0131	0.0131	-0.0268	-0.0080	-0.0489	0.0528
TotalAll	0.0462	0.0462	-0.0437	0.0138	-0.0988	0.0944
ElevMADMedian	0.8719	0.8719	0.7425	0.9591	-0.0038	-0.3757
ElevMADMode	0.7867	0.7867	0.7021	0.8825	0.0185	-0.4028
CanopyReliefRatio	0.1232	0.1232	-0.4108	-0.0288	-0.9502	0.4255
ElevQuadraticMean	0.5357	0.5357	-0.0707	0.3812	-0.6189	0.3077
ElevCubicMean	0.5795	0.5795	-0.0158	0.4239	-0.5909	0.2826

	ElevAAD	ElevL1	ElevL2	ElevL3	ElevL4	ElevLCV
TotalReturns	0.5071	0.4975	0.5211	-0.2614	0.3148	0.2482
ElevMin	-0.2670	0.4227	-0.2577	-0.1568	0.1068	-0.5686
ElevMax	0.7115	0.8592	0.7364	-0.3796	0.4228	0.2377
ElevMean	0.4182	1.0000	0.4435	-0.6023	0.4308	-0.1719
ElevMode	0.3290	0.8969	0.3536	-0.6901	0.4502	-0.2234
ElevStdDev	0.9881	0.4781	0.9938	-0.2910	0.2243	0.7329
ElevVar	0.9881	0.4781	0.9938	-0.2909	0.2243	0.7329
ElevCV	0.7947	-0.1388	0.7786	0.1780	-0.1084	0.9944
ElevIQ	0.9502	0.3254	0.9360	-0.1444	-0.1002	0.7971
ElevSkew	-0.0873	-0.6453	-0.1100	0.8949	-0.4124	0.3784
ElevKurtosis	-0.2473	0.3412	-0.2063	-0.2412	0.7973	-0.4707
ElevAAD	1.0000	0.4182	0.9969	-0.2408	0.1127	0.7806
ElevL1	0.4182	1.0000	0.4435	-0.6023	0.4308	-0.1719
ElevL2	0.9969	0.4435	1.0000	-0.2580	0.1636	0.7627
ElevL3	-0.2408	-0.6023	-0.2580	1.0000	-0.3365	0.2082
ElevL4	0.1127	0.4308	0.1636	-0.3365	1.0000	-0.1699
ElevLCV	0.7806	-0.1719	0.7627	0.2082	-0.1699	1.0000
ElevLSkewness	-0.1736	-0.5888	-0.1920	0.9538	-0.3742	0.2679
ElevLKurtosis	-0.3133	0.2518	-0.2635	-0.2126	0.8411	-0.5041
ElevP01	-0.1581	0.6296	-0.1426	-0.2684	0.2187	-0.5798
ElevP05	-0.0676	0.7745	-0.0448	-0.3769	0.3506	-0.5684
ElevP10	-0.0008	0.8437	0.0273	-0.4643	0.4506	-0.5416
ElevP20	0.1294	0.9185	0.1609	-0.5849	0.5466	-0.4518
ElevP25	0.1853	0.9401	0.2167	-0.6269	0.5546	-0.4042
ElevP30	0.2386	0.9570	0.2692	-0.6575	0.5431	-0.3547
ElevP40	0.3352	0.9786	0.3635	-0.6902	0.4891	-0.2588
ElevP50	0.4195	0.9871	0.4441	-0.6873	0.4267	-0.1706
ElevP60	0.4901	0.9846	0.5119	-0.6555	0.3764	-0.0927
ElevP70	0.5553	0.9735	0.5754	-0.6078	0.3424	-0.0157
ElevP75	0.5858	0.9648	0.6057	-0.5789	0.3365	0.0230
ElevP80	0.6159	0.9534	0.6360	-0.5470	0.3383	0.0629
ElevP90	0.6691	0.9241	0.6910	-0.4742	0.3681	0.1422
ElevP95	0.6944	0.8997	0.7178	-0.4290	0.3947	0.1882
ElevP99	0.7091	0.8712	0.7337	-0.3891	0.4175	0.2262
Return1Above3	0.4902	0.4929	0.5042	-0.2579	0.3171	0.2334
Return2Above3	0.7439	0.4273	0.7540	-0.2742	0.2406	0.5103
Return3Above3	0.0502	0.0488	0.0501	-0.0300	0.0196	0.0153
Return4Above3	ND	ND	ND	ND	ND	ND
Return5Above3	ND	ND	ND	ND	ND	ND
Return6Above3	ND	ND	ND	ND	ND	ND
Return7Above3	ND	ND	ND	ND	ND	ND
Return8Above3	ND	ND	ND	ND	ND	ND
Return9Above3	ND	ND	ND	ND	ND	ND
OtherReturnAbove3	ND	ND	ND	ND	ND	ND
PercentFirstAbove3	0.5889	0.5422	0.6074	-0.2716	0.3359	0.3166
PercentAllAbove3	0.6088	0.5110	0.6260	-0.2537	0.3196	0.3582

	ElevAAD	ElevL1	ElevL2	ElevL3	ElevL4	ElevLCV
AllDivFirstTimes100	0.6049	0.5436	0.6232	-0.2727	0.3295	0.3326
FirstAbove3	0.4902	0.4929	0.5042	-0.2579	0.3171	0.2334
AllAbove3	0.5071	0.4975	0.5211	-0.2614	0.3148	0.2482
PercentAboveMean	0.5859	0.6217	0.6065	-0.4663	0.3819	0.2415
PercentFirstAboveMode	0.4168	0.3184	0.4303	0.0386	0.2399	0.3007
PercentAllAboveMean	0.5983	0.5951	0.6180	-0.4488	0.3709	0.2722
PercentAllAboveMode	0.4208	0.2859	0.4331	0.0603	0.2257	0.3270
AllAboveMeanDivByFirstTimes100	0.5910	0.6201	0.6116	-0.4616	0.3799	0.2482
AllAboveModeDivByFirstTimes100	0.4203	0.3152	0.4336	0.0439	0.2368	0.3066
FirstAboveMean	0.5103	0.5665	0.5266	-0.4155	0.3545	0.1909
FirstAboveMode	0.3892	0.3376	0.4003	-0.0218	0.2510	0.2470
AllAboveMean	0.5145	0.5655	0.5308	-0.4124	0.3533	0.1962
AllAboveMode	0.3934	0.3350	0.4044	-0.0164	0.2477	0.2535
TotalFirst	0.0073	0.0193	0.0018	-0.0658	0.0015	-0.0394
TotalAll	0.0350	0.1023	0.0320	-0.1033	0.0406	-0.0588
ElevMADMedian	0.9138	0.3386	0.9091	-0.1460	-0.0670	0.7573
ElevMADMode	0.8308	0.2693	0.8268	-0.1160	-0.0982	0.7217
CanopyReliefRatio	0.0583	0.6968	0.0797	-0.8237	0.3891	-0.4407
ElevQuadraticMean	0.4768	0.9959	0.5014	-0.5865	0.4171	-0.1043
ElevCubicMean	0.5215	0.9871	0.5455	-0.5654	0.4082	-0.0497

	ElevLSkewness	ElevLKurtosis	ElevP01	ElevP05	ElevP10
TotalReturns	-0.2345	0.0825	0.0553	0.2168	0.2893
ElevMin	-0.2156	0.2136	0.8811	0.7530	0.6791
ElevMax	-0.3474	0.1187	0.3273	0.4797	0.5583
ElevMean	-0.5888	0.2518	0.6296	0.7745	0.8437
ElevMode	-0.6634	0.2886	0.5846	0.7159	0.7864
ElevStdDev	-0.2308	-0.1956	-0.1351	-0.0211	0.0615
ElevVar	-0.2308	-0.1956	-0.1351	-0.0211	0.0615
ElevCV	0.2355	-0.4446	-0.5821	-0.5575	-0.5196
ElevIQ	-0.0720	-0.5095	-0.1642	-0.0993	-0.0617
ElevSkew	0.9519	-0.3609	-0.4159	-0.5489	-0.6291
ElevKurtosis	-0.3002	0.8966	0.2931	0.4283	0.5005
ElevAAD	-0.1736	-0.3133	-0.1581	-0.0676	-0.0008
ElevL1	-0.5888	0.2518	0.6296	0.7745	0.8437
ElevL2	-0.1920	-0.2635	-0.1426	-0.0448	0.0273
ElevL3	0.9538	-0.2126	-0.2684	-0.3769	-0.4643
ElevL4	-0.3742	0.8411	0.2187	0.3506	0.4506
ElevLCV	0.2679	-0.5041	-0.5798	-0.5684	-0.5416
ElevLSkewness	1.0000	-0.2785	-0.3228	-0.4316	-0.5151
ElevLKurtosis	-0.2785	1.0000	0.2778	0.3708	0.4381
ElevP01	-0.3228	0.2778	1.0000	0.9175	0.8546
ElevP05	-0.4316	0.3708	0.9175	1.0000	0.9638
ElevP10	-0.5151	0.4381	0.8546	0.9638	1.0000
ElevP20	-0.6177	0.4646	0.7674	0.8947	0.9544
ElevP25	-0.6492	0.4426	0.7358	0.8668	0.9300
ElevP30	-0.6681	0.4091	0.7051	0.8397	0.9062
ElevP40	-0.6793	0.3273	0.6521	0.7911	0.8615
ElevP50	-0.6632	0.2452	0.6039	0.7470	0.8193
ElevP60	-0.6283	0.1769	0.5598	0.7058	0.7796
ElevP70	-0.5792	0.1211	0.5145	0.6617	0.7370
ElevP75	-0.5502	0.1018	0.4919	0.6395	0.7154
ElevP80	-0.5177	0.0886	0.4681	0.6155	0.6914
ElevP90	-0.4439	0.0903	0.4155	0.5637	0.6402
ElevP95	-0.3978	0.1026	0.3804	0.5289	0.6057
ElevP99	-0.3568	0.1154	0.3436	0.4936	0.5712
Return1Above3	-0.2332	0.0915	0.0598	0.2214	0.2932
Return2Above3	-0.2206	-0.0922	-0.0756	0.0484	0.1209
Return3Above3	-0.0260	-0.0071	0.0151	0.0235	0.0265
Return4Above3	ND	ND	ND	ND	ND
Return5Above3	ND	ND	ND	ND	ND
Return6Above3	ND	ND	ND	ND	ND
Return7Above3	ND	ND	ND	ND	ND
Return8Above3	ND	ND	ND	ND	ND
Return9Above3	ND	ND	ND	ND	ND
OtherReturnAbove3	ND	ND	ND	ND	ND
PercentFirstAbove3	-0.2344	0.0579	0.0633	0.2245	0.3011
PercentAllAbove3	-0.2145	0.0324	0.0194	0.1799	0.2575

	ElevLSkewness	ElevLKurtosis	ElevP01	ElevP05	ElevP10
AllDivFirstTimes100	-0.2337	0.0462	0.0569	0.2170	0.2939
FirstAbove3	-0.2332	0.0915	0.0598	0.2214	0.2932
AllAbove3	-0.2345	0.0825	0.0553	0.2168	0.2893
PercentAboveMean	-0.4252	0.1068	0.1077	0.2789	0.3700
PercentFirstAboveMode	0.0354	0.0472	-0.0070	0.1189	0.1677
PercentAllAboveMean	-0.4072	0.0889	0.0722	0.2440	0.3356
PercentAllAboveMode	0.0585	0.0301	-0.0425	0.0815	0.1301
AllAboveMeanDivByFirstTimes100	-0.4205	0.1030	0.1043	0.2752	0.3660
AllAboveModeDivByFirstTimes100	0.0405	0.0431	-0.0101	0.1149	0.1633
FirstAboveMean	-0.3877	0.1188	0.0955	0.2658	0.3497
FirstAboveMode	-0.0195	0.0763	-0.0063	0.1325	0.1853
AllAboveMean	-0.3845	0.1161	0.0929	0.2630	0.3468
AllAboveMode	-0.0144	0.0718	-0.0093	0.1288	0.1812
TotalFirst	-0.0556	0.0078	-0.0410	-0.0127	-0.0063
TotalAll	-0.0947	0.0374	0.0232	0.0639	0.0734
ElevMADMedian	-0.0750	-0.4671	-0.1376	-0.0650	-0.0252
ElevMADMode	-0.0559	-0.4686	-0.1441	-0.0931	-0.0630
CanopyReliefRatio	-0.8827	0.3540	0.5332	0.6585	0.7206
ElevQuadraticMean	-0.5687	0.2178	0.5828	0.7308	0.8036
ElevCubicMean	-0.5453	0.1923	0.5456	0.6951	0.7698

	ElevP20	ElevP25	ElevP30	ElevP40	ElevP50	ElevP60	ElevP70
TotalReturns	0.3742	0.4006	0.4251	0.4634	0.4879	0.5092	0.5296
ElevMin	0.5794	0.5434	0.5093	0.4525	0.4016	0.3569	0.3121
ElevMax	0.6625	0.6985	0.7316	0.7869	0.8314	0.8672	0.8999
ElevMean	0.9185	0.9401	0.9570	0.9786	0.9871	0.9846	0.9735
ElevMode	0.8624	0.8860	0.9012	0.9164	0.9107	0.8922	0.8644
ElevStdDev	0.2009	0.2567	0.3085	0.4004	0.4783	0.5436	0.6047
ElevVar	0.2009	0.2567	0.3085	0.4004	0.4783	0.5436	0.6047
ElevCV	-0.4181	-0.3685	-0.3184	-0.2233	-0.1367	-0.0606	0.0149
ElevIQ	0.0287	0.0768	0.1323	0.2357	0.3254	0.4011	0.4723
ElevSkew	-0.7066	-0.7242	-0.7312	-0.7244	-0.6998	-0.6627	-0.6128
ElevKurtosis	0.5261	0.5062	0.4762	0.4026	0.3300	0.2691	0.2167
ElevAAD	0.1294	0.1853	0.2386	0.3352	0.4195	0.4901	0.5553
ElevL1	0.9185	0.9401	0.9570	0.9786	0.9871	0.9846	0.9735
ElevL2	0.1609	0.2167	0.2692	0.3635	0.4441	0.5119	0.5754
ElevL3	-0.5849	-0.6269	-0.6575	-0.6902	-0.6873	-0.6555	-0.6078
ElevL4	0.5466	0.5546	0.5431	0.4891	0.4267	0.3764	0.3424
ElevLCV	-0.4518	-0.4042	-0.3547	-0.2588	-0.1706	-0.0927	-0.0157
ElevLSkewness	-0.6177	-0.6492	-0.6681	-0.6793	-0.6632	-0.6283	-0.5792
ElevLKurtosis	0.4646	0.4426	0.4091	0.3273	0.2452	0.1769	0.1211
ElevP01	0.7674	0.7358	0.7051	0.6521	0.6039	0.5598	0.5145
ElevP05	0.8947	0.8668	0.8397	0.7911	0.7470	0.7058	0.6617
ElevP10	0.9544	0.9300	0.9062	0.8615	0.8193	0.7796	0.7370
ElevP20	1.0000	0.9903	0.9752	0.9404	0.9040	0.8690	0.8307
ElevP25	0.9903	1.0000	0.9923	0.9644	0.9313	0.8983	0.8621
ElevP30	0.9752	0.9923	1.0000	0.9822	0.9533	0.9230	0.8892
ElevP40	0.9404	0.9644	0.9822	1.0000	0.9847	0.9616	0.9337
ElevP50	0.9040	0.9313	0.9533	0.9847	1.0000	0.9881	0.9665
ElevP60	0.8690	0.8983	0.9230	0.9616	0.9881	1.0000	0.9887
ElevP70	0.8307	0.8621	0.8892	0.9337	0.9665	0.9887	1.0000
ElevP75	0.8105	0.8427	0.8709	0.9176	0.9528	0.9784	0.9962
ElevP80	0.7881	0.8211	0.8505	0.8993	0.9369	0.9653	0.9874
ElevP90	0.7404	0.7749	0.8062	0.8588	0.9006	0.9335	0.9615
ElevP95	0.7078	0.7432	0.7755	0.8298	0.8734	0.9080	0.9387
ElevP99	0.6749	0.7108	0.7436	0.7988	0.8433	0.8790	0.9116
Return1Above3	0.3762	0.4014	0.4247	0.4608	0.4832	0.5030	0.5220
Return2Above3	0.2285	0.2699	0.3084	0.3756	0.4282	0.4724	0.5135
Return3Above3	0.0352	0.0395	0.0443	0.0455	0.0462	0.0465	0.0529
Return4Above3	ND	ND	ND	ND	ND	ND	ND
Return5Above3	ND	ND	ND	ND	ND	ND	ND
Return6Above3	ND	ND	ND	ND	ND	ND	ND
Return7Above3	ND	ND	ND	ND	ND	ND	ND
Return8Above3	ND	ND	ND	ND	ND	ND	ND
Return9Above3	ND	ND	ND	ND	ND	ND	ND
OtherReturnAbove3	ND	ND	ND	ND	ND	ND	ND
PercentFirstAbove3	0.3940	0.4251	0.4542	0.5000	0.5308	0.5569	0.5812
PercentAllAbove3	0.3538	0.3867	0.4176	0.4666	0.5009	0.5299	0.5571

	ElevP20	ElevP25	ElevP30	ElevP40	ElevP50	ElevP60	ElevP70
AllDivFirstTimes100	0.3885	0.4207	0.4510	0.4992	0.5324	0.5603	0.5860
FirstAbove3	0.3762	0.4014	0.4247	0.4608	0.4832	0.5030	0.5220
AllAbove3	0.3742	0.4006	0.4251	0.4634	0.4879	0.5092	0.5296
PercentAboveMean	0.4836	0.5219	0.5556	0.6059	0.6348	0.6511	0.6598
PercentFirstAboveMode	0.2150	0.2263	0.2391	0.2615	0.2841	0.3106	0.3438
PercentAllAboveMean	0.4515	0.4910	0.5259	0.5781	0.6091	0.6271	0.6380
PercentAllAboveMode	0.1784	0.1903	0.2038	0.2276	0.2522	0.2804	0.3156
AllAboveMeanDivByFirstTimes100	0.4798	0.5183	0.5522	0.6031	0.6328	0.6497	0.6593
AllAboveModeDivByFirstTimes100	0.2103	0.2216	0.2344	0.2573	0.2805	0.3077	0.3415
FirstAboveMean	0.4509	0.4832	0.5114	0.5533	0.5760	0.5897	0.5978
FirstAboveMode	0.2389	0.2519	0.2660	0.2891	0.3088	0.3313	0.3602
AllAboveMean	0.4482	0.4806	0.5090	0.5514	0.5747	0.5889	0.5976
AllAboveMode	0.2345	0.2475	0.2617	0.2852	0.3057	0.3290	0.3587
TotalFirst	0.0089	0.0132	0.0175	0.0234	0.0231	0.0242	0.0253
TotalAll	0.0902	0.0944	0.0984	0.1043	0.1034	0.1036	0.1033
ElevMADMedian	0.0637	0.1085	0.1565	0.2519	0.3404	0.4130	0.4763
ElevMADMode	0.0174	0.0580	0.1022	0.1908	0.2761	0.3424	0.3988
CanopyReliefRatio	0.7703	0.7780	0.7775	0.7615	0.7332	0.6964	0.6488
ElevQuadraticMean	0.8867	0.9123	0.9333	0.9637	0.9817	0.9883	0.9856
ElevCubicMean	0.8581	0.8863	0.9101	0.9465	0.9708	0.9844	0.9891

	ElevP75	ElevP80	ElevP90	ElevP95	ElevP99	Return1Above3
TotalReturns	0.5403	0.5486	0.5749	0.5879	0.6118	0.9999
ElevMin	0.2901	0.2671	0.2166	0.1824	0.1429	-0.1708
ElevMax	0.9153	0.9302	0.9624	0.9798	0.9953	0.6198
ElevMean	0.9648	0.9534	0.9241	0.8997	0.8712	0.4929
ElevMode	0.8477	0.8281	0.7871	0.7597	0.7321	0.4658
ElevStdDev	0.6339	0.6633	0.7177	0.7449	0.7615	0.5201
ElevVar	0.6339	0.6633	0.7176	0.7449	0.7615	0.5201
ElevCV	0.0530	0.0925	0.1723	0.2192	0.2592	0.2568
ElevIQ	0.5049	0.5313	0.5735	0.5936	0.6066	0.4418
ElevSkew	-0.5835	-0.5505	-0.4735	-0.4231	-0.3777	-0.2537
ElevKurtosis	0.1971	0.1816	0.1767	0.1870	0.2043	0.2215
ElevAAD	0.5858	0.6159	0.6691	0.6944	0.7091	0.4902
ElevL1	0.9648	0.9534	0.9241	0.8997	0.8712	0.4929
ElevL2	0.6057	0.6360	0.6910	0.7178	0.7337	0.5042
ElevL3	-0.5789	-0.5470	-0.4742	-0.4290	-0.3891	-0.2579
ElevL4	0.3365	0.3383	0.3681	0.3947	0.4175	0.3171
ElevLCV	0.0230	0.0629	0.1422	0.1882	0.2262	0.2334
ElevLSkewness	-0.5502	-0.5177	-0.4439	-0.3978	-0.3568	-0.2332
ElevLKurtosis	0.1018	0.0886	0.0903	0.1026	0.1154	0.0915
ElevP01	0.4919	0.4681	0.4155	0.3804	0.3436	0.0598
ElevP05	0.6395	0.6155	0.5637	0.5289	0.4936	0.2214
ElevP10	0.7154	0.6914	0.6402	0.6057	0.5712	0.2932
ElevP20	0.8105	0.7881	0.7404	0.7078	0.6749	0.3762
ElevP25	0.8427	0.8211	0.7749	0.7432	0.7108	0.4014
ElevP30	0.8709	0.8505	0.8062	0.7755	0.7436	0.4247
ElevP40	0.9176	0.8993	0.8588	0.8298	0.7988	0.4608
ElevP50	0.9528	0.9369	0.9006	0.8734	0.8433	0.4832
ElevP60	0.9784	0.9653	0.9335	0.9080	0.8790	0.5030
ElevP70	0.9962	0.9874	0.9615	0.9387	0.9116	0.5220
ElevP75	1.0000	0.9953	0.9736	0.9526	0.9268	0.5320
ElevP80	0.9953	1.0000	0.9852	0.9660	0.9416	0.5397
ElevP90	0.9736	0.9852	1.0000	0.9911	0.9725	0.5650
ElevP95	0.9526	0.9660	0.9911	1.0000	0.9885	0.5775
ElevP99	0.9268	0.9416	0.9725	0.9885	1.0000	0.6012
Return1Above3	0.5320	0.5397	0.5650	0.5775	0.6012	1.0000
Return2Above3	0.5341	0.5536	0.5959	0.6171	0.6423	0.8489
Return3Above3	0.0545	0.0548	0.0555	0.0561	0.0560	0.0413
Return4Above3	ND	ND	ND	ND	ND	ND
Return5Above3	ND	ND	ND	ND	ND	ND
Return6Above3	ND	ND	ND	ND	ND	ND
Return7Above3	ND	ND	ND	ND	ND	ND
Return8Above3	ND	ND	ND	ND	ND	ND
Return9Above3	ND	ND	ND	ND	ND	ND
OtherReturnAbove3	ND	ND	ND	ND	ND	ND
PercentFirstAbove3	0.5947	0.6056	0.6362	0.6540	0.6809	0.9766
PercentAllAbove3	0.5721	0.5846	0.6185	0.6385	0.6678	0.9768

	ElevP75	ElevP80	ElevP90	ElevP95	ElevP99	Return1Above3
AllDivFirstTimes100	0.6002	0.6118	0.6435	0.6618	0.6888	0.9762
FirstAbove3	0.5320	0.5397	0.5650	0.5775	0.6012	1.0000
AllAbove3	0.5403	0.5486	0.5749	0.5879	0.6118	0.9999
PercentAboveMean	0.6640	0.6652	0.6759	0.6828	0.6994	0.8111
PercentFirstAboveMode	0.3630	0.3814	0.4256	0.4493	0.4799	0.6265
PercentAllAboveMean	0.6435	0.6459	0.6596	0.6684	0.6873	0.8171
PercentAllAboveMode	0.3358	0.3553	0.4020	0.4273	0.4596	0.6203
AllAboveMeanDivByFirstTimes100	0.6639	0.6655	0.6774	0.6848	0.7017	0.8118
AllAboveModeDivByFirstTimes100	0.3611	0.3799	0.4249	0.4489	0.4798	0.6243
FirstAboveMean	0.6014	0.6020	0.6126	0.6173	0.6337	0.9914
FirstAboveMode	0.3763	0.3914	0.4308	0.4499	0.4783	0.9722
AllAboveMean	0.6016	0.6026	0.6140	0.6190	0.6357	0.9915
AllAboveMode	0.3752	0.3908	0.4309	0.4504	0.4791	0.9718
TotalFirst	0.0249	0.0249	0.0254	0.0224	0.0226	-0.0786
TotalAll	0.1022	0.1010	0.0998	0.0956	0.0949	0.0314
ElevMADMedian	0.5041	0.5300	0.5744	0.5954	0.6098	0.4588
ElevMADMode	0.4239	0.4479	0.4896	0.5092	0.5215	0.3588
CanopyReliefRatio	0.6211	0.5899	0.5144	0.4611	0.4042	0.2439
ElevQuadraticMean	0.9808	0.9731	0.9502	0.9290	0.9027	0.5112
ElevCubicMean	0.9880	0.9839	0.9674	0.9495	0.9255	0.5249

	Return2Above3	Return3Above3	Return4Above3
TotalReturns	0.8527	0.0416	ND
ElevMin	-0.2406	0.0032	ND
ElevMax	0.6575	0.0561	ND
ElevMean	0.4273	0.0488	ND
ElevMode	0.3901	0.0421	ND
ElevStdDev	0.7569	0.0510	ND
ElevVar	0.7569	0.0510	ND
ElevCV	0.5283	0.0181	ND
ElevIQ	0.6891	0.0429	ND
ElevSkew	-0.1651	-0.0165	ND
ElevKurtosis	-0.0282	-0.0019	ND
ElevAAD	0.7439	0.0502	ND
ElevL1	0.4273	0.0488	ND
ElevL2	0.7540	0.0501	ND
ElevL3	-0.2742	-0.0300	ND
ElevL4	0.2406	0.0196	ND
ElevLCV	0.5103	0.0153	ND
ElevLSkewness	-0.2206	-0.0260	ND
ElevLKurtosis	-0.0922	-0.0071	ND
ElevP01	-0.0756	0.0151	ND
ElevP05	0.0484	0.0235	ND
ElevP10	0.1209	0.0265	ND
ElevP20	0.2285	0.0352	ND
ElevP25	0.2699	0.0395	ND
ElevP30	0.3084	0.0443	ND
ElevP40	0.3756	0.0455	ND
ElevP50	0.4282	0.0462	ND
ElevP60	0.4724	0.0465	ND
ElevP70	0.5135	0.0529	ND
ElevP75	0.5341	0.0545	ND
ElevP80	0.5536	0.0548	ND
ElevP90	0.5959	0.0555	ND
ElevP95	0.6171	0.0561	ND
ElevP99	0.6423	0.0560	ND
Return1Above3	0.8489	0.0413	ND
Return2Above3	1.0000	0.0480	ND
Return3Above3	0.0480	1.0000	ND
Return4Above3	ND	ND	ND
Return5Above3	ND	ND	ND
Return6Above3	ND	ND	ND
Return7Above3	ND	ND	ND
Return8Above3	ND	ND	ND
Return9Above3	ND	ND	ND
OtherReturnAbove3	ND	ND	ND
PercentFirstAbove3	0.8557	0.0421	ND
PercentAllAbove3	0.8595	0.0416	ND

	Return2Above3	Return3Above3	Return4Above3
AllDivFirstTimes100	0.8594	0.0427	ND
FirstAbove3	0.8489	0.0413	ND
AllAbove3	0.8527	0.0416	ND
PercentAboveMean	0.7565	0.0469	ND
PercentFirstAboveMode	0.5342	0.0228	ND
PercentAllAboveMean	0.7647	0.0447	ND
PercentAllAboveMode	0.5329	0.0204	ND
AllAboveMeanDivByFirstTimes100	0.7614	0.0469	ND
AllAboveModeDivByFirstTimes100	0.5375	0.0227	ND
FirstAboveMean	0.8574	0.0431	ND
FirstAboveMode	0.8237	0.0363	ND
AllAboveMean	0.8582	0.0431	ND
AllAboveMode	0.8245	0.0362	ND
TotalFirst	-0.0867	0.0038	ND
TotalAll	0.0093	0.0098	ND
ElevMADMedian	0.6932	0.0354	ND
ElevMADMode	0.6034	0.0238	ND
CanopyReliefRatio	0.1356	0.0208	ND
ElevQuadraticMean	0.4667	0.0505	ND
ElevCubicMean	0.4965	0.0519	ND

	Return5Above3	Return6Above3	Return7Above3
TotalReturns	ND	ND	ND
ElevMin	ND	ND	ND
ElevMax	ND	ND	ND
ElevMean	ND	ND	ND
ElevMode	ND	ND	ND
ElevStdDev	ND	ND	ND
ElevVar	ND	ND	ND
ElevCV	ND	ND	ND
ElevIQ	ND	ND	ND
ElevSkew	ND	ND	ND
ElevKurtosis	ND	ND	ND
ElevAAD	ND	ND	ND
ElevL1	ND	ND	ND
ElevL2	ND	ND	ND
ElevL3	ND	ND	ND
ElevL4	ND	ND	ND
ElevLCV	ND	ND	ND
ElevLSkewness	ND	ND	ND
ElevLKurtosis	ND	ND	ND
ElevP01	ND	ND	ND
ElevP05	ND	ND	ND
ElevP10	ND	ND	ND
ElevP20	ND	ND	ND
ElevP25	ND	ND	ND
ElevP30	ND	ND	ND
ElevP40	ND	ND	ND
ElevP50	ND	ND	ND
ElevP60	ND	ND	ND
ElevP70	ND	ND	ND
ElevP75	ND	ND	ND
ElevP80	ND	ND	ND
ElevP90	ND	ND	ND
ElevP95	ND	ND	ND
ElevP99	ND	ND	ND
Return1Above3	ND	ND	ND
Return2Above3	ND	ND	ND
Return3Above3	ND	ND	ND
Return4Above3	ND	ND	ND
Return5Above3	ND	ND	ND
Return6Above3	ND	ND	ND
Return7Above3	ND	ND	ND
Return8Above3	ND	ND	ND
Return9Above3	ND	ND	ND
OtherReturnAbove3	ND	ND	ND
PercentFirstAbove3	ND	ND	ND
PercentAllAbove3	ND	ND	ND

	Return5Above3	Return6Above3	Return7Above3
AllDivFirstTimes100	ND	ND	ND
FirstAbove3	ND	ND	ND
AllAbove3	ND	ND	ND
PercentAboveMean	ND	ND	ND
PercentFirstAboveMode	ND	ND	ND
PercentAllAboveMean	ND	ND	ND
PercentAllAboveMode	ND	ND	ND
AllAboveMeanDivByFirstTimes100	ND	ND	ND
AllAboveModeDivByFirstTimes100	ND	ND	ND
FirstAboveMean	ND	ND	ND
FirstAboveMode	ND	ND	ND
AllAboveMean	ND	ND	ND
AllAboveMode	ND	ND	ND
TotalFirst	ND	ND	ND
TotalAll	ND	ND	ND
ElevMADMedian	ND	ND	ND
ElevMADMode	ND	ND	ND
CanopyReliefRatio	ND	ND	ND
ElevQuadraticMean	ND	ND	ND
ElevCubicMean	ND	ND	ND

	Return8Above3	Return9Above3	OtherReturnAbove3
TotalReturns	ND	ND	ND
ElevMin	ND	ND	ND
ElevMax	ND	ND	ND
ElevMean	ND	ND	ND
ElevMode	ND	ND	ND
ElevStdDev	ND	ND	ND
ElevVar	ND	ND	ND
ElevCV	ND	ND	ND
ElevIQ	ND	ND	ND
ElevSkew	ND	ND	ND
ElevKurtosis	ND	ND	ND
ElevAAD	ND	ND	ND
ElevL1	ND	ND	ND
ElevL2	ND	ND	ND
ElevL3	ND	ND	ND
ElevL4	ND	ND	ND
ElevLCV	ND	ND	ND
ElevLSkewness	ND	ND	ND
ElevLKurtosis	ND	ND	ND
ElevP01	ND	ND	ND
ElevP05	ND	ND	ND
ElevP10	ND	ND	ND
ElevP20	ND	ND	ND
ElevP25	ND	ND	ND
ElevP30	ND	ND	ND
ElevP40	ND	ND	ND
ElevP50	ND	ND	ND
ElevP60	ND	ND	ND
ElevP70	ND	ND	ND
ElevP75	ND	ND	ND
ElevP80	ND	ND	ND
ElevP90	ND	ND	ND
ElevP95	ND	ND	ND
ElevP99	ND	ND	ND
Return1Above3	ND	ND	ND
Return2Above3	ND	ND	ND
Return3Above3	ND	ND	ND
Return4Above3	ND	ND	ND
Return5Above3	ND	ND	ND
Return6Above3	ND	ND	ND
Return7Above3	ND	ND	ND
Return8Above3	ND	ND	ND
Return9Above3	ND	ND	ND
OtherReturnAbove3	ND	ND	ND
PercentFirstAbove3	ND	ND	ND
PercentAllAbove3	ND	ND	ND

	Return8Above3	Return9Above3	OtherReturnAbove3
AllDivFirstTimes100	ND	ND	ND
FirstAbove3	ND	ND	ND
AllAbove3	ND	ND	ND
PercentAboveMean	ND	ND	ND
PercentFirstAboveMode	ND	ND	ND
PercentAllAboveMean	ND	ND	ND
PercentAllAboveMode	ND	ND	ND
AllAboveMeanDivByFirstTimes100	ND	ND	ND
AllAboveModeDivByFirstTimes100	ND	ND	ND
FirstAboveMean	ND	ND	ND
FirstAboveMode	ND	ND	ND
AllAboveMean	ND	ND	ND
AllAboveMode	ND	ND	ND
TotalFirst	ND	ND	ND
TotalAll	ND	ND	ND
ElevMADMedian	ND	ND	ND
ElevMADMode	ND	ND	ND
CanopyReliefRatio	ND	ND	ND
ElevQuadraticMean	ND	ND	ND
ElevCubicMean	ND	ND	ND

	PercentFirstAbove3	PercentAllAbove3	AllDivFirstTimes100
TotalReturns	0.9776	0.9779	0.9774
ElevMin	-0.1503	-0.1896	-0.1554
ElevMax	0.6997	0.6875	0.7075
ElevMean	0.5422	0.5110	0.5436
ElevMode	0.4999	0.4709	0.4989
ElevStdDev	0.6167	0.6331	0.6320
ElevVar	0.6167	0.6331	0.6320
ElevCV	0.3348	0.3755	0.3507
ElevIQ	0.5398	0.5628	0.5556
ElevSkew	-0.2409	-0.2136	-0.2368
ElevKurtosis	0.1656	0.1402	0.1528
ElevAAD	0.5889	0.6088	0.6049
ElevL1	0.5422	0.5110	0.5436
ElevL2	0.6074	0.6260	0.6232
ElevL3	-0.2716	-0.2537	-0.2727
ElevL4	0.3359	0.3196	0.3295
ElevLCV	0.3166	0.3582	0.3326
ElevLSkewness	-0.2344	-0.2145	-0.2337
ElevLKurtosis	0.0579	0.0324	0.0462
ElevP01	0.0633	0.0194	0.0569
ElevP05	0.2245	0.1799	0.2170
ElevP10	0.3011	0.2575	0.2939
ElevP20	0.3940	0.3538	0.3885
ElevP25	0.4251	0.3867	0.4207
ElevP30	0.4542	0.4176	0.4510
ElevP40	0.5000	0.4666	0.4992
ElevP50	0.5308	0.5009	0.5324
ElevP60	0.5569	0.5299	0.5603
ElevP70	0.5812	0.5571	0.5860
ElevP75	0.5947	0.5721	0.6002
ElevP80	0.6056	0.5846	0.6118
ElevP90	0.6362	0.6185	0.6435
ElevP95	0.6540	0.6385	0.6618
ElevP99	0.6809	0.6678	0.6888
Return1Above3	0.9766	0.9768	0.9762
Return2Above3	0.8557	0.8595	0.8594
Return3Above3	0.0421	0.0416	0.0427
Return4Above3	ND	ND	ND
Return5Above3	ND	ND	ND
Return6Above3	ND	ND	ND
Return7Above3	ND	ND	ND
Return8Above3	ND	ND	ND
Return9Above3	ND	ND	ND
OtherReturnAbove3	ND	ND	ND
PercentFirstAbove3	1.0000	0.9995	0.9999
PercentAllAbove3	0.9995	1.0000	0.9995

	PercentFirstAbove3	PercentAllAbove3	AllDivFirstTimes100
AllDivFirstTimes100	0.9999	0.9995	1.0000
FirstAbove3	0.9766	0.9768	0.9762
AllAbove3	0.9776	0.9779	0.9774
PercentAboveMean	0.9644	0.9574	0.9651
PercentFirstAboveMode	0.7532	0.7547	0.7531
PercentAllAboveMean	0.9670	0.9659	0.9673
PercentAllAboveMode	0.7418	0.7482	0.7415
AllAboveMeanDivByFirstTimes100	0.9658	0.9591	0.9668
AllAboveModeDivByFirstTimes100	0.7506	0.7525	0.7509
FirstAboveMean	0.9712	0.9710	0.9710
FirstAboveMode	0.9517	0.9522	0.9514
AllAboveMean	0.9714	0.9712	0.9713
AllAboveMode	0.9516	0.9521	0.9513
TotalFirst	-0.1941	-0.1927	-0.1948
TotalAll	-0.0866	-0.0869	-0.0871
ElevMADMedian	0.5681	0.5901	0.5831
ElevMADMode	0.4701	0.4921	0.4844
CanopyReliefRatio	0.2243	0.1910	0.2197
ElevQuadraticMean	0.5666	0.5381	0.5695
ElevCubicMean	0.5847	0.5584	0.5886

	FirstAbove3	AllAbove3	PercentAboveMean
TotalReturns	0.9999	1.0000	0.8188
ElevMin	-0.1708	-0.1753	-0.1095
ElevMax	0.6198	0.6304	0.7149
ElevMean	0.4929	0.4975	0.6217
ElevMode	0.4658	0.4686	0.6026
ElevStdDev	0.5201	0.5365	0.6241
ElevVar	0.5201	0.5365	0.6241
ElevCV	0.2568	0.2714	0.2668
ElevIQ	0.4418	0.4580	0.5154
ElevSkew	-0.2537	-0.2518	-0.4181
ElevKurtosis	0.2215	0.2111	0.2089
ElevAAD	0.4902	0.5071	0.5859
ElevL1	0.4929	0.4975	0.6217
ElevL2	0.5042	0.5211	0.6065
ElevL3	-0.2579	-0.2614	-0.4663
ElevL4	0.3171	0.3148	0.3819
ElevLCV	0.2334	0.2482	0.2415
ElevLSkewness	-0.2332	-0.2345	-0.4252
ElevLKurtosis	0.0915	0.0825	0.1068
ElevP01	0.0598	0.0553	0.1077
ElevP05	0.2214	0.2168	0.2789
ElevP10	0.2932	0.2893	0.3700
ElevP20	0.3762	0.3742	0.4836
ElevP25	0.4014	0.4006	0.5219
ElevP30	0.4247	0.4251	0.5556
ElevP40	0.4608	0.4634	0.6059
ElevP50	0.4832	0.4879	0.6348
ElevP60	0.5030	0.5092	0.6511
ElevP70	0.5220	0.5296	0.6598
ElevP75	0.5320	0.5403	0.6640
ElevP80	0.5397	0.5486	0.6652
ElevP90	0.5650	0.5749	0.6759
ElevP95	0.5775	0.5879	0.6828
ElevP99	0.6012	0.6118	0.6994
Return1Above3	1.0000	0.9999	0.8111
Return2Above3	0.8489	0.8527	0.7565
Return3Above3	0.0413	0.0416	0.0469
Return4Above3	ND	ND	ND
Return5Above3	ND	ND	ND
Return6Above3	ND	ND	ND
Return7Above3	ND	ND	ND
Return8Above3	ND	ND	ND
Return9Above3	ND	ND	ND
OtherReturnAbove3	ND	ND	ND
PercentFirstAbove3	0.9766	0.9776	0.9644
PercentAllAbove3	0.9768	0.9779	0.9574

	FirstAbove3	AllAbove3	PercentAboveMean
AllDivFirstTimes100	0.9762	0.9774	0.9651
FirstAbove3	1.0000	0.9999	0.8111
AllAbove3	0.9999	1.0000	0.8188
PercentAboveMean	0.8111	0.8188	1.0000
PercentFirstAboveMode	0.6265	0.6303	0.6802
PercentAllAboveMean	0.8171	0.8247	0.9970
PercentAllAboveMode	0.6203	0.6240	0.6644
AllAboveMeanDivByFirstTimes100	0.8118	0.8198	0.9998
AllAboveModeDivByFirstTimes100	0.6243	0.6283	0.6768
FirstAboveMean	0.9914	0.9915	0.8616
FirstAboveMode	0.9722	0.9720	0.6346
AllAboveMean	0.9915	0.9916	0.8619
AllAboveMode	0.9718	0.9717	0.6328
TotalFirst	-0.0786	-0.0807	-0.0448
TotalAll	0.0314	0.0294	0.0237
ElevMADMedian	0.4588	0.4745	0.5420
ElevMADMode	0.3588	0.3738	0.4430
CanopyReliefRatio	0.2439	0.2416	0.3777
ElevQuadraticMean	0.5112	0.5171	0.6403
ElevCubicMean	0.5249	0.5317	0.6517

	PercentFirstAboveMode	PercentAllAboveMean
TotalReturns	0.6303	0.8247
ElevMin	-0.1537	-0.1422
ElevMax	0.4952	0.7039
ElevMean	0.3184	0.5951
ElevMode	0.0896	0.5784
ElevStdDev	0.4348	0.6338
ElevVar	0.4348	0.6338
ElevCV	0.3122	0.2966
ElevIQ	0.3953	0.5309
ElevSkew	-0.0229	-0.3950
ElevKurtosis	0.1500	0.1912
ElevAAD	0.4168	0.5983
ElevL1	0.3184	0.5951
ElevL2	0.4303	0.6180
ElevL3	0.0386	-0.4488
ElevL4	0.2399	0.3709
ElevLCV	0.3007	0.2722
ElevLSkewness	0.0354	-0.4072
ElevLKurtosis	0.0472	0.0889
ElevP01	-0.0070	0.0722
ElevP05	0.1189	0.2440
ElevP10	0.1677	0.3356
ElevP20	0.2150	0.4515
ElevP25	0.2263	0.4910
ElevP30	0.2391	0.5259
ElevP40	0.2615	0.5781
ElevP50	0.2841	0.6091
ElevP60	0.3106	0.6271
ElevP70	0.3438	0.6380
ElevP75	0.3630	0.6435
ElevP80	0.3814	0.6459
ElevP90	0.4256	0.6596
ElevP95	0.4493	0.6684
ElevP99	0.4799	0.6873
Return1Above3	0.6265	0.8171
Return2Above3	0.5342	0.7647
Return3Above3	0.0228	0.0447
Return4Above3	ND	ND
Return5Above3	ND	ND
Return6Above3	ND	ND
Return7Above3	ND	ND
Return8Above3	ND	ND
Return9Above3	ND	ND
OtherReturnAbove3	ND	ND
PercentFirstAbove3	0.7532	0.9670
PercentAllAbove3	0.7547	0.9659

	PercentFirstAboveMode	PercentAllAboveMean
AllDivFirstTimes100	0.7531	0.9673
FirstAbove3	0.6265	0.8171
AllAbove3	0.6303	0.8247
PercentAboveMean	0.6802	0.9970
PercentFirstAboveMode	1.0000	0.6843
PercentAllAboveMean	0.6843	1.0000
PercentAllAboveMode	0.9975	0.6729
AllAboveMeanDivByFirstTimes100	0.6822	0.9972
AllAboveModeDivByFirstTimes100	0.9998	0.6811
FirstAboveMean	0.5856	0.8641
FirstAboveMode	0.8571	0.6416
AllAboveMean	0.5872	0.8647
AllAboveMode	0.8593	0.6399
TotalFirst	-0.1210	-0.0364
TotalAll	-0.0656	0.0249
ElevMADMedian	0.4279	0.5572
ElevMADMode	0.3980	0.4585
CanopyReliefRatio	0.0149	0.3500
ElevQuadraticMean	0.3410	0.6156
ElevCubicMean	0.3602	0.6286

	PercentAllAboveMode	AllAbMeanDivByFirstTimes100
TotalReturns	0.6240	0.8198
ElevMin	-0.1838	-0.1126
ElevMax	0.4755	0.7174
ElevMean	0.2859	0.6201
ElevMode	0.0568	0.5997
ElevStdDev	0.4361	0.6289
ElevVar	0.4361	0.6289
ElevCV	0.3377	0.2734
ElevIQ	0.4024	0.5206
ElevSkew	0.0044	-0.4127
ElevKurtosis	0.1330	0.2048
ElevAAD	0.4208	0.5910
ElevL1	0.2859	0.6201
ElevL2	0.4331	0.6116
ElevL3	0.0603	-0.4616
ElevL4	0.2257	0.3799
ElevLCV	0.3270	0.2482
ElevLSkewness	0.0585	-0.4205
ElevLKurtosis	0.0301	0.1030
ElevP01	-0.0425	0.1043
ElevP05	0.0815	0.2752
ElevP10	0.1301	0.3660
ElevP20	0.1784	0.4798
ElevP25	0.1903	0.5183
ElevP30	0.2038	0.5522
ElevP40	0.2276	0.6031
ElevP50	0.2522	0.6328
ElevP60	0.2804	0.6497
ElevP70	0.3156	0.6593
ElevP75	0.3358	0.6639
ElevP80	0.3553	0.6655
ElevP90	0.4020	0.6774
ElevP95	0.4273	0.6848
ElevP99	0.4596	0.7017
Return1Above3	0.6203	0.8118
Return2Above3	0.5329	0.7614
Return3Above3	0.0204	0.0469
Return4Above3	ND	ND
Return5Above3	ND	ND
Return6Above3	ND	ND
Return7Above3	ND	ND
Return8Above3	ND	ND
Return9Above3	ND	ND
OtherReturnAbove3	ND	ND
PercentFirstAbove3	0.7418	0.9658
PercentAllAbove3	0.7482	0.9591

	PercentAllAboveMode	AllAboveMeanDivByFirstTimes100
AllDivFirstTimes100	0.7415	0.9668
FirstAbove3	0.6203	0.8118
AllAbove3	0.6240	0.8198
PercentAboveMean	0.6644	0.9998
PercentFirstAboveMode	0.9975	0.6822
PercentAllAboveMean	0.6729	0.9972
PercentAllAboveMode	1.0000	0.6667
AllAboveMeanDivByFirstTimes100	0.6667	1.0000
AllAboveModeDivByFirstTimes100	0.9977	0.6790
FirstAboveMean	0.5756	0.8614
FirstAboveMode	0.8586	0.6362
AllAboveMean	0.5774	0.8619
AllAboveMode	0.8610	0.6345
TotalFirst	-0.1140	-0.0447
TotalAll	-0.0658	0.0236
ElevMADMedian	0.4336	0.5472
ElevMADMode	0.4056	0.4481
CanopyReliefRatio	-0.0161	0.3724
ElevQuadraticMean	0.3102	0.6393
ElevCubicMean	0.3308	0.6512

	AllAboveModeDivByFirstTimes100	FirstAboveMean
TotalReturns	0.6283	0.9915
ElevMin	-0.1559	-0.1393
ElevMax	0.4952	0.6499
ElevMean	0.3152	0.5665
ElevMode	0.0845	0.5555
ElevStdDev	0.4378	0.5473
ElevVar	0.4378	0.5473
ElevCV	0.3179	0.2185
ElevIQ	0.3993	0.4464
ElevSkew	-0.0173	-0.3935
ElevKurtosis	0.1457	0.2412
ElevAAD	0.4203	0.5103
ElevL1	0.3152	0.5665
ElevL2	0.4336	0.5266
ElevL3	0.0439	-0.4155
ElevL4	0.2368	0.3545
ElevLCV	0.3066	0.1909
ElevLSkewness	0.0405	-0.3877
ElevLKurtosis	0.0431	0.1188
ElevP01	-0.0101	0.0955
ElevP05	0.1149	0.2658
ElevP10	0.1633	0.3497
ElevP20	0.2103	0.4509
ElevP25	0.2216	0.4832
ElevP30	0.2344	0.5114
ElevP40	0.2573	0.5533
ElevP50	0.2805	0.5760
ElevP60	0.3077	0.5897
ElevP70	0.3415	0.5978
ElevP75	0.3611	0.6014
ElevP80	0.3799	0.6020
ElevP90	0.4249	0.6126
ElevP95	0.4489	0.6173
ElevP99	0.4798	0.6337
Return1Above3	0.6243	0.9914
Return2Above3	0.5375	0.8574
Return3Above3	0.0227	0.0431
Return4Above3	ND	ND
Return5Above3	ND	ND
Return6Above3	ND	ND
Return7Above3	ND	ND
Return8Above3	ND	ND
Return9Above3	ND	ND
OtherReturnAbove3	ND	ND
PercentFirstAbove3	0.7506	0.9712
PercentAllAbove3	0.7525	0.9710

	AllAboveModeDivByFirstTimes100	FirstAboveMean
AllDivFirstTimes100	0.7509	0.9710
FirstAbove3	0.6243	0.9914
AllAbove3	0.6283	0.9915
PercentAboveMean	0.6768	0.8616
PercentFirstAboveMode	0.9998	0.5856
PercentAllAboveMean	0.6811	0.8641
PercentAllAboveMode	0.9977	0.5756
AllAboveMeanDivByFirstTimes100	0.6790	0.8614
AllAboveModeDivByFirstTimes100	1.0000	0.5826
FirstAboveMean	0.5826	1.0000
FirstAboveMode	0.8565	0.9702
AllAboveMean	0.5845	1.0000
AllAboveMode	0.8590	0.9697
TotalFirst	-0.1214	-0.0824
TotalAll	-0.0663	0.0288
ElevMADMedian	0.4318	0.4642
ElevMADMode	0.4021	0.3631
CanopyReliefRatio	0.0094	0.3649
ElevQuadraticMean	0.3383	0.5816
ElevCubicMean	0.3579	0.5911

	FirstAboveMode	AllAboveMean	AllAboveMode	TotalFirst
TotalReturns	0.9720	0.9916	0.9717	-0.0807
ElevMin	-0.1904	-0.1418	-0.1926	-0.1134
ElevMax	0.4950	0.6521	0.4959	0.0260
ElevMean	0.3376	0.5655	0.3350	0.0193
ElevMode	0.1493	0.5535	0.1439	0.0453
ElevStdDev	0.4129	0.5513	0.4166	0.0131
ElevVar	0.4129	0.5513	0.4166	0.0131
ElevCV	0.2658	0.2237	0.2720	-0.0268
ElevIQ	0.3570	0.4506	0.3618	-0.0080
ElevSkew	-0.0761	-0.3897	-0.0705	-0.0489
ElevKurtosis	0.1984	0.2383	0.1936	0.0528
ElevAAD	0.3892	0.5145	0.3934	0.0073
ElevL1	0.3376	0.5655	0.3350	0.0193
ElevL2	0.4003	0.5308	0.4044	0.0018
ElevL3	-0.0218	-0.4124	-0.0164	-0.0658
ElevL4	0.2510	0.3533	0.2477	0.0015
ElevLCV	0.2470	0.1962	0.2535	-0.0394
ElevLSkewness	-0.0195	-0.3845	-0.0144	-0.0556
ElevLKurtosis	0.0763	0.1161	0.0718	0.0078
ElevP01	-0.0063	0.0929	-0.0093	-0.0410
ElevP05	0.1325	0.2630	0.1288	-0.0127
ElevP10	0.1853	0.3468	0.1812	-0.0063
ElevP20	0.2389	0.4482	0.2345	0.0089
ElevP25	0.2519	0.4806	0.2475	0.0132
ElevP30	0.2660	0.5090	0.2617	0.0175
ElevP40	0.2891	0.5514	0.2852	0.0234
ElevP50	0.3088	0.5747	0.3057	0.0231
ElevP60	0.3313	0.5889	0.3290	0.0242
ElevP70	0.3602	0.5976	0.3587	0.0253
ElevP75	0.3763	0.6016	0.3752	0.0249
ElevP80	0.3914	0.6026	0.3908	0.0249
ElevP90	0.4308	0.6140	0.4309	0.0254
ElevP95	0.4499	0.6190	0.4504	0.0224
ElevP99	0.4783	0.6357	0.4791	0.0226
Return1Above3	0.9722	0.9915	0.9718	-0.0786
Return2Above3	0.8237	0.8582	0.8245	-0.0867
Return3Above3	0.0363	0.0431	0.0362	0.0038
Return4Above3	ND	ND	ND	ND
Return5Above3	ND	ND	ND	ND
Return6Above3	ND	ND	ND	ND
Return7Above3	ND	ND	ND	ND
Return8Above3	ND	ND	ND	ND
Return9Above3	ND	ND	ND	ND
OtherReturnAbove3	ND	ND	ND	ND
PercentFirstAbove3	0.9517	0.9714	0.9516	-0.1941
PercentAllAbove3	0.9522	0.9712	0.9521	-0.1927

	FirstAboveMode	AllAboveMean	AllAboveMode	TotalFirst
AllDivFirstTimes100	0.9514	0.9713	0.9513	-0.1948
FirstAbove3	0.9722	0.9915	0.9718	-0.0786
AllAbove3	0.9720	0.9916	0.9717	-0.0807
PercentAboveMean	0.6346	0.8619	0.6328	-0.0448
PercentFirstAboveMode	0.8571	0.5872	0.8593	-0.1210
PercentAllAboveMean	0.6416	0.8647	0.6399	-0.0364
PercentAllAboveMode	0.8586	0.5774	0.8610	-0.1140
AllAboveMeanDivByFirstTimes100	0.6362	0.8619	0.6345	-0.0447
AllAboveModeDivByFirstTimes100	0.8565	0.5845	0.8590	-0.1214
FirstAboveMean	0.9702	1.0000	0.9697	-0.0824
FirstAboveMode	1.0000	0.9703	1.0000	-0.0945
AllAboveMean	0.9703	1.0000	0.9699	-0.0825
AllAboveMode	1.0000	0.9699	1.0000	-0.0954
TotalFirst	-0.0945	-0.0825	-0.0954	1.0000
TotalAll	0.0136	0.0286	0.0127	0.9887
ElevMADMedian	0.3764	0.4683	0.3811	-0.0297
ElevMADMode	0.3266	0.3672	0.3317	-0.0565
CanopyReliefRatio	0.0717	0.3612	0.0663	0.0604
ElevQuadraticMean	0.3576	0.5811	0.3556	0.0204
ElevCubicMean	0.3743	0.5910	0.3728	0.0214

	TotalAll	ElevMADMedian	ElevMADMode	CanopyReliefRatio
TotalReturns	0.0294	0.4745	0.3738	0.2416
ElevMin	-0.0701	-0.2377	-0.2182	0.3742
ElevMax	0.0981	0.6143	0.5244	0.3837
ElevMean	0.1023	0.3386	0.2693	0.6968
ElevMode	0.1188	0.2509	0.1413	0.7192
ElevStdDev	0.0462	0.8719	0.7867	0.1232
ElevVar	0.0462	0.8719	0.7867	0.1232
ElevCV	-0.0437	0.7425	0.7021	-0.4108
ElevIQ	0.0138	0.9591	0.8825	-0.0288
ElevSkew	-0.0988	-0.0038	0.0185	-0.9502
ElevKurtosis	0.0944	-0.3757	-0.4028	0.4255
ElevAAD	0.0350	0.9138	0.8308	0.0583
ElevL1	0.1023	0.3386	0.2693	0.6968
ElevL2	0.0320	0.9091	0.8268	0.0797
ElevL3	-0.1033	-0.1460	-0.1160	-0.8237
ElevL4	0.0406	-0.0670	-0.0982	0.3891
ElevLCV	-0.0588	0.7573	0.7217	-0.4407
ElevLSkewness	-0.0947	-0.0750	-0.0559	-0.8827
ElevLKurtosis	0.0374	-0.4671	-0.4686	0.3540
ElevP01	0.0232	-0.1376	-0.1441	0.5332
ElevP05	0.0639	-0.0650	-0.0931	0.6585
ElevP10	0.0734	-0.0252	-0.0630	0.7206
ElevP20	0.0902	0.0637	0.0174	0.7703
ElevP25	0.0944	0.1085	0.0580	0.7780
ElevP30	0.0984	0.1565	0.1022	0.7775
ElevP40	0.1043	0.2519	0.1908	0.7615
ElevP50	0.1034	0.3404	0.2761	0.7332
ElevP60	0.1036	0.4130	0.3424	0.6964
ElevP70	0.1033	0.4763	0.3988	0.6488
ElevP75	0.1022	0.5041	0.4239	0.6211
ElevP80	0.1010	0.5300	0.4479	0.5899
ElevP90	0.0998	0.5744	0.4896	0.5144
ElevP95	0.0956	0.5954	0.5092	0.4611
ElevP99	0.0949	0.6098	0.5215	0.4042
Return1Above3	0.0314	0.4588	0.3588	0.2439
Return2Above3	0.0093	0.6932	0.6034	0.1356
Return3Above3	0.0098	0.0354	0.0238	0.0208
Return4Above3	ND	ND	ND	ND
Return5Above3	ND	ND	ND	ND
Return6Above3	ND	ND	ND	ND
Return7Above3	ND	ND	ND	ND
Return8Above3	ND	ND	ND	ND
Return9Above3	ND	ND	ND	ND
OtherReturnAbove3	ND	ND	ND	ND
PercentFirstAbove3	-0.0866	0.5681	0.4701	0.2243
PercentAllAbove3	-0.0869	0.5901	0.4921	0.1910

	TotalAll	ElevMADMedian	ElevMADMode	CanopyReliefRatio
AllDivFirstTimes100	-0.0871	0.5831	0.4844	0.2197
FirstAbove3	0.0314	0.4588	0.3588	0.2439
AllAbove3	0.0294	0.4745	0.3738	0.2416
PercentAboveMean	0.0237	0.5420	0.4430	0.3777
PercentFirstAboveMode	-0.0656	0.4279	0.3980	0.0149
PercentAllAboveMean	0.0249	0.5572	0.4585	0.3500
PercentAllAboveMode	-0.0658	0.4336	0.4056	-0.0161
AllAboveMeanDivByFirstTimes100	0.0236	0.5472	0.4481	0.3724
AllAboveModeDivByFirstTimes100	-0.0663	0.4318	0.4021	0.0094
FirstAboveMean	0.0288	0.4642	0.3631	0.3649
FirstAboveMode	0.0136	0.3764	0.3266	0.0717
AllAboveMean	0.0286	0.4683	0.3672	0.3612
AllAboveMode	0.0127	0.3811	0.3317	0.0663
TotalFirst	0.9887	-0.0297	-0.0565	0.0604
TotalAll	1.0000	-0.0046	-0.0401	0.1164
ElevMADMedian	-0.0046	1.0000	0.9278	-0.0138
ElevMADMode	-0.0401	0.9278	1.0000	-0.0410
CanopyReliefRatio	0.1164	-0.0138	-0.0410	1.0000
ElevQuadraticMean	0.1021	0.3901	0.3168	0.6658
ElevCubicMean	0.1018	0.4295	0.3532	0.6351

	ElevQuadraticMean	ElevCubicMean
TotalReturns	0.5171	0.5317
ElevMin	0.3761	0.3394
ElevMax	0.8911	0.9143
ElevMean	0.9959	0.9871
ElevMode	0.8839	0.8681
ElevStdDev	0.5357	0.5795
ElevVar	0.5357	0.5795
ElevCV	-0.0707	-0.0158
ElevIQ	0.3812	0.4239
ElevSkew	-0.6189	-0.5909
ElevKurtosis	0.3077	0.2826
ElevAAD	0.4768	0.5215
ElevL1	0.9959	0.9871
ElevL2	0.5014	0.5455
ElevL3	-0.5865	-0.5654
ElevL4	0.4171	0.4082
ElevLCV	-0.1043	-0.0497
ElevLSkewness	-0.5687	-0.5453
ElevLKurtosis	0.2178	0.1923
ElevP01	0.5828	0.5456
ElevP05	0.7308	0.6951
ElevP10	0.8036	0.7698
ElevP20	0.8867	0.8581
ElevP25	0.9123	0.8863
ElevP30	0.9333	0.9101
ElevP40	0.9637	0.9465
ElevP50	0.9817	0.9708
ElevP60	0.9883	0.9844
ElevP70	0.9856	0.9891
ElevP75	0.9808	0.9880
ElevP80	0.9731	0.9839
ElevP90	0.9502	0.9674
ElevP95	0.9290	0.9495
ElevP99	0.9027	0.9255
Return1Above3	0.5112	0.5249
Return2Above3	0.4667	0.4965
Return3Above3	0.0505	0.0519
Return4Above3	ND	ND
Return5Above3	ND	ND
Return6Above3	ND	ND
Return7Above3	ND	ND
Return8Above3	ND	ND
Return9Above3	ND	ND
OtherReturnAbove3	ND	ND
PercentFirstAbove3	0.5666	0.5847
PercentAllAbove3	0.5381	0.5584

	ElevQuadraticMean	ElevCubicMean
AllDivFirstTimes100	0.5695	0.5886
FirstAbove3	0.5112	0.5249
AllAbove3	0.5171	0.5317
PercentAboveMean	0.6403	0.6517
PercentFirstAboveMode	0.3410	0.3602
PercentAllAboveMean	0.6156	0.6286
PercentAllAboveMode	0.3102	0.3308
AllAboveMeanDivByFirstTimes100	0.6393	0.6512
AllAboveModeDivByFirstTimes100	0.3383	0.3579
FirstAboveMean	0.5816	0.5911
FirstAboveMode	0.3576	0.3743
AllAboveMean	0.5811	0.5910
AllAboveMode	0.3556	0.3728
TotalFirst	0.0204	0.0214
TotalAll	0.1021	0.1018
ElevMADMedian	0.3901	0.4295
ElevMADMode	0.3168	0.3532
CanopyReliefRatio	0.6658	0.6351
ElevQuadraticMean	1.0000	0.9973
ElevCubicMean	0.9973	1.0000

Table A2: Correlation matrix of potential model parameters.

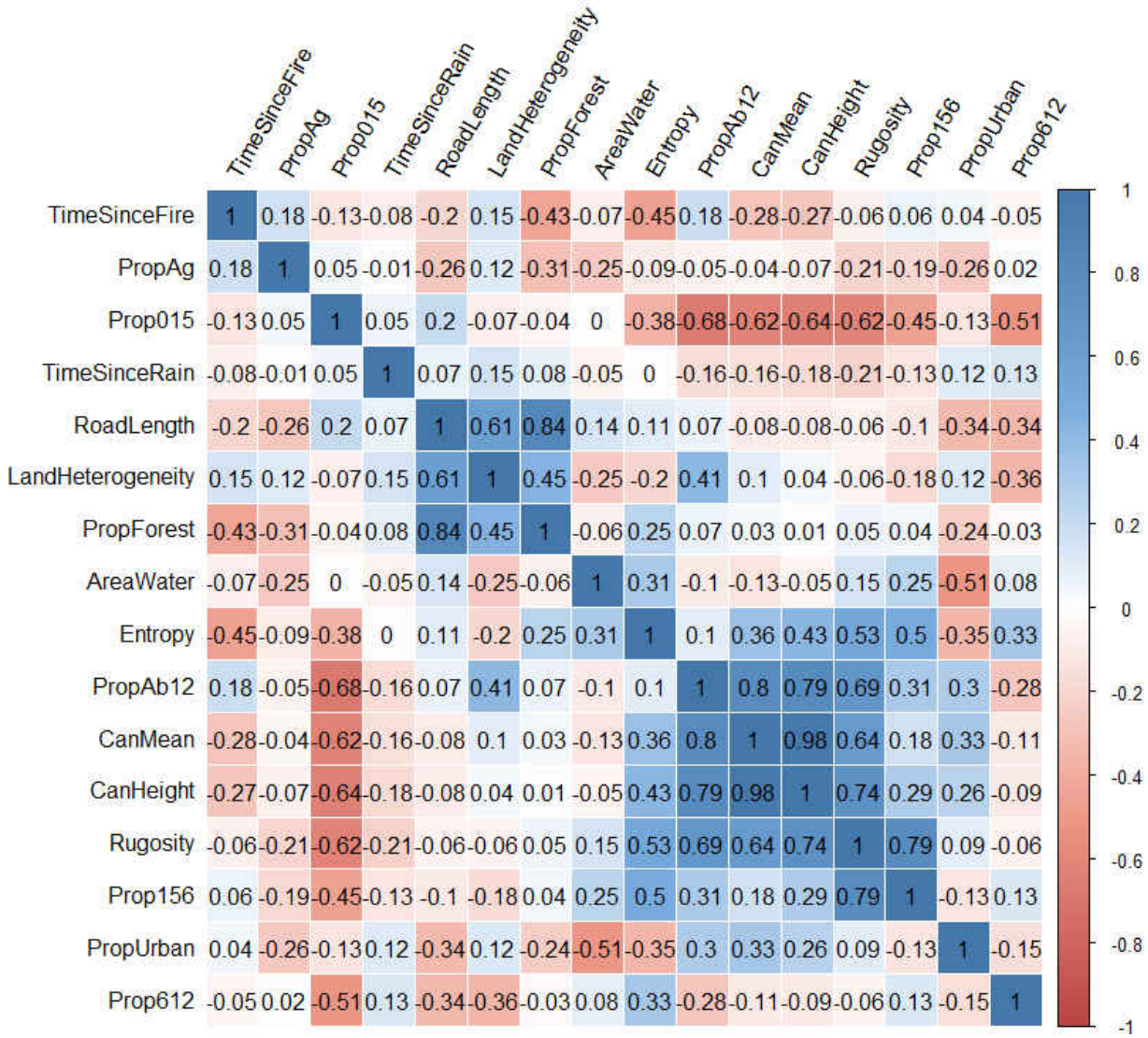

APPENDIX B: SITE AND MODEL SELECTION PARAMETERS

Table B1: Site selection parameters for k-means clustering analysis.

Parameter	Ecological Significance
Minimum canopy height	Height (m) of the lowest canopy tree within 5x5 m site
Maximum canopy height	Height (m) of the tallest canopy tree within 5x5 m site
Mean canopy height	Arithmetic mean (m) of all of the heights of the canopy trees within 5x5 m site
Standard deviation of canopy height	The rugosity of the canopy within 5x5 m site (m)
Canopy height skew	The skew of the canopy heights within 5x5 m site
Canopy height kurtosis	The kurtosis of the canopy heights within 5x5 m site
Percent of returns above 3 m	The structural clutter above 3 m.
Proportion of binned returns (0-0.5 m, 0.5-1.5 m, 1.5-3 m, 3-6 m., 6-9 m, 9-12 m, above 12 m)	Bins of vertical forest structure; used to calculate entropy and describe the height profiles of each 5x5 m site

Table B2: Complete parameter set for model development.

Parameter	Ecological Significance
LiDAR	
Mean canopy height	Mean height (m) of the canopy within 5x5 m area
Rugosity	Standard deviation (m) of canopy height within 5x5 m area
Percent of returns above 3 m	Percentage of LiDAR returns above 3 m.
Proportion of LiDAR returns (0-1.5 m)	Proportion of returns that were shrubby and herbaceous understory within 5x5 m area
Proportion of LiDAR returns (1.5-6 m)	Proportion of returns that were within forest midstory in 5x5 m area
Proportion of LiDAR returns (6-12 m)	Proportion of returns that were upper midstory to canopy within 5x5 m area
Proportion of LiDAR returns (above 12 m)	Proportion of tall canopy returns within 5x5 m area
Entropy	Vertical diversity of forest layers (Jost diversity of binned LiDAR returns)
Landscape and Disturbance	
Time since fire	Time, in months, since last prescribed burn (unburned areas were marked as 50 years since fire)
Area of water	Total area (ha) of lakes and ponds within 1.5 km buffer
Service road length	Total length of service roads (m) within area of 1.5 km buffer inside of OSBS
Landscape heterogeneity	Jost diversity of k-means clusters within 1.5 km buffer bounded by OSBS
Proportion of urban lands	Proportion of lands classified by FLUCCS as urban inside of 1.5 km buffer
Proportion of agricultural lands	Proportion of lands classified by FLUCCS as agricultural or pasture inside of 1.5 km buffer
Proportion of forested lands	Proportion of lands classified by FLUCCS as forested inside of 1.5 km buffer
Proportion of non-forested lands	Proportion of lands classified by FLUCCS as non-forested inside of 1.5 km buffer
Season and Weather	
Season	Sampling season (early or late summer)
Time since rain	Time, in days, since last rain

APPENDIX C: SAMPLING TIMES

Table C1: Sampling weeks for each site (cluster 1 - red, 2 - orange, 3 - yellow, 4 - purple, 5 - blue, 6 - green) corresponding to Figure 3A.

Site	June 15-21	June 29-July 4	July 5-11	Aug 10-16	Aug 17-23	Aug 24-30	Aug 31-Sept 6
1							
6				*			*
11							
14							
15							
18							
27							
29							
30							**
33				*			*
35							
39							
42							
49							
50							
55						*	*
60							
66							

* Half of the week was sampled due to equipment issues
** Only one week total sampled at this site

APPENDIX D: COMPLETE MODEL SELECTION RESULTS

Table D1: AIC table for bat abundance models.

	K	AICc	ΔAICc	AICcWt	Cum.Wt	LL
Model 8	12	1922.6	0.0	0.42	0.42	-949.3
Model 9	13	1923.3	0.7	0.30	0.72	-948.6
Model 10	13	1923.5	0.9	0.27	0.99	-948.8
Model 5	8	1936.4	13.8	0.01	1.00	-960.2
Model 6	9	1937.1	14.5	0.00	1.00	-959.6
Model 7	9	1937.8	15.2	0.00	1.00	-959.9
Model 1	8	1944.4	21.8	0.00	1.00	-964.2
Model 3	5	1945.1	22.5	0.00	1.00	-967.6
Model 2	9	1946.0	23.4	0.00	1.00	-964.0
Model 4	6	1946.4	23.8	0.00	1.00	-967.2

Table D2: AIC table for bat community diversity models.

	K	AICc	ΔAICc	AICc.Wt	Cum.Wt	LL
Model 10	13	-14.86	0.00	1	1	21.66
Model 8	13	7.13	21.99	0	1	10.67
Model 9	13	22.02	36.88	0	1	3.22
Model 7	12	38.62	53.47	0	1	-6.26
Model 5	9	83.74	98.60	0	1	-32.28
Model 6	10	85.92	100.78	0	1	-32.23
Model 1	8	98.39	113.25	0	1	-40.73
Model 2	9	100.19	115.05	0	1	-40.50
Model 4	6	105.65	120.50	0	1	-46.55
Model 3	5	111.08	125.94	0	1	-50.35

Table D3: AIC table for logistic models, evening bat (*N. humeralis*).

	K	AICc	ΔAICc	AICcWt	Cum.Wt	LL
Model 6	9	136.71	0.00	0.98	0.98	-58.81
Model 4	5	145.83	9.11	0.01	0.99	-67.73
Model 2	8	146.01	9.30	0.01	1.00	-64.57
Model 10	12	149.79	13.08	0.00	1.00	-61.93
Model 7	11	150.47	13.75	0.00	1.00	-63.42
Model 8	12	152.65	15.94	0.00	1.00	-63.36
Model 9	12	152.74	16.03	0.00	1.00	-63.40
Model 5	8	155.21	18.49	0.00	1.00	-69.17
Model 1	7	159.94	23.22	0.00	1.00	-72.63
Model 3	4	164.20	27.49	0.00	1.00	-77.98

Table D4: AIC table for logistic models, tricolored bat (*P. subflavus*).

	K	AICc	ΔAIC	AICc.Wt	Cum.Wt	LL
Model 10	12	185.63	0.00	0.84	0.84	-79.84
Model 8	12	190.51	4.88	0.07	0.92	-82.29
Model 7	11	191.93	6.30	0.04	0.95	-84.15
Model 5	8	192.97	7.34	0.02	0.97	-88.05
Model 9	12	194.18	8.56	0.01	0.99	-84.12
Model 6	9	194.51	8.89	0.01	1.00	-87.71
Model 1	7	196.64	11.01	0.00	1.00	-90.98
Model 2	8	198.72	13.10	0.00	1.00	-90.93
Model 4	5	217.55	31.92	0.00	1.00	-103.60
Model 3	4	227.86	42.24	0.00	1.00	-109.81

Table D5: AIC table for logistic models, southeastern myotis (*M austroriparius*).

	K	AICc	ΔAIC	AICc.Wt	Cum.Wt	LL
Model 5	8	130.65	0.00	0.50	0.50	-56.89
Model 6	9	132.80	2.14	0.17	0.67	-56.85
Model 7	11	133.41	2.76	0.12	0.79	-54.89
Model 9	12	135.28	4.62	0.05	0.84	-54.67
Model 1	7	135.45	4.79	0.05	0.88	-60.39
Model 8	12	135.46	4.81	0.04	0.93	-54.76
Model 10	12	135.52	4.87	0.04	0.97	-54.79
Model 2	8	137.39	6.73	0.02	0.99	-60.26
Model 4	5	138.44	7.79	0.01	1.00	-64.04
Model 3	4	152.87	22.21	0.00	1.00	-72.32

Table D6: AIC table for logistic models, big brown bat (*E. fuscus*).

	K	AICc	ΔAIC	AICc.Wt	Cum.Wt	LL
Model 7	11	91.46	0.00	0.33	0.33	-33.92
Model 10	12	91.54	0.08	0.32	0.65	-32.80
Model 9	12	92.10	0.64	0.24	0.89	-33.08
Model 8	12	93.65	2.19	0.11	1.00	-33.85
Model 5	8	101.27	9.81	0.00	1.00	-42.20
Model 6	9	102.41	10.95	0.00	1.00	-41.66
Model 3	4	121.61	30.15	0.00	1.00	-56.69
Model 2	8	121.97	30.51	0.00	1.00	-52.55
Model 1	7	122.11	30.65	0.00	1.00	-53.72
Model 4	5	123.70	32.24	0.00	1.00	-56.67

Table D7: Results for second most informative logistic model, big brown bat (*E. fuscus*).

	Estimate	Std. Error	z value	Pr(>|z|)
Intercept	72.87	31.88	2.286	<0.05
Mean canopy height	-0.6002	0.2553	-2.351	<0.05
Entropy	3.971	1.655	2.400	<0.05
Rugosity	-4.878	3.582	-1.362	0.173
Proportion of returns (0-1.5 m)	-22.33	9.650	-2.314	<0.05
Proportion of returns (1.5-6 m)	6.747	73.21	0.092	0.927
Proportion of returns (6-12 m)	-28.86	10.57	-2.730	<0.01
Proportion of urban lands	-7.297	1.020	-0.715	0.474
Water area	-0.0447	0.0321	-1.393	0.164
Length of service roads	-0.0019	0.0012	-1.636	0.102
Landscape heterogeneity	-9.070	5.280	-1.718	0.086
ServiceRoadLength:LandscapeHeterogeneity	0.0003	0.0002	1.307	0.191

Table D8: Results for third most informative logistic model, big brown bat (*E. fuscus*).

	Estimate	Std. Error	z value	Pr(>|z|)
Intercept	70.84	33.37	2.123	<0.05
Mean canopy height	-0.6656	0.2620	-2.540	<0.05
Entropy	3.927	1.670	2.351	<0.05
Rugosity	-4.785	2.983	-1.604	0.109
Proportion of returns (0-1.5 m)	-23.34	10.76	-2.170	<0.05
Proportion of returns (1.5-6 m)	8.111	50.78	0.160	0.873
Proportion of returns (6-12 m)	-29.75	11.07	-2.687	<0.01
Proportion of urban lands	-8.957	10.17	-0.880	0.379
Landscape heterogeneity	-7.648	4.569	-1.674	0.094
Water area	-0.4123	0.3162	-1.304	0.192
Length of service roads	-0.0006	0.0002	-2.617	<0.01
LandscapeHeterogeneity:WaterArea	0.0813	0.0675	1.206	0.228

APPENDIX E: R CODE

Correlation Matrices

```
##Model selection parameter matrix
##Set the working directory
setwd("G:/Thesis/Data")

##Read the data
bat.data<-read.csv("BatMasterDataFINALWorking2.csv", header=T)
names(bat.data)

##Load packages
library(corrplot)
library(grDevices)

##Subset the parameters being considered for model selection
bat.subset<-
subset(bat.data,select=c(CanHeight,CanopyMean,Rugosity,Prop015,Prop156,Prop612,PropAb12,TimeSi
nceRain,TimeSinceFire,PercentWater,RoadLength,LandHeterogeneity,PropUrban,PropAg,PropForest,En
tropy))

##Run the correlation matrix
mcor<-cor(bat.subset)

##Graph the correlation matrix
col<-colorRampPalette(c("#BB4444","#EE9988","#FFFFFF","#77AADD","#4477AA"))
corrplot(mcor,method="shade",shade.col=NA,tl.col="black",tl.srt=60,col=col(200),addCoef.col="black",
addcolorlabel="no",order="AOE")
```

K Means Clustering and Site Selection

```
##set directory
setwd("G:/Project_Home/Products/Collated Metrics")
getwd()

##read data
osdata<-read.csv("OSAllGIS.csv", header=T)
names(osdata)

##calculate the return counts
osbsdata$SumX<-
(X0to3+X3to6+X6to9+X9to12+X12to15+X15to18+X18to21+X21to24+X24to27+X27to30+X30to33)

attach(osdata)
names(osbsdata)
```

```
##add columns with percent returns by bin
osbsdata$P0to3<-(X0to3/SumX)
osbsdata$P3to6<-(X3to6/SumX)
osbsdata$P6to9<-(X6to9/SumX)
osbsdata$P9to12<-(X9to12/SumX)
osbsdata$P12to15<-(X12to15/SumX)
osbsdata$P15to18<-(X15to18/SumX)
osbsdata$P18to21<-(X18to21/SumX)
osbsdata$P21to24<-(X21to24/SumX)
osbsdata$P24to27<-(X24to27/SumX)
osbsdata$P27to30<-(X27to30/SumX)
osbsdata$P30to33<-(X30to33/SumX)

##Detach and reattach data to ensure new columns are present
detach(osbsdata)
attach(osbsdata)

names(osbsdata)

##write table with percentages
write.table(unclass(osbsdata), "OSBSdatatrunc.txt", sep=",", col.names=T, row.names=F)

##run kmeans without total return count (this was messing up the clusters with remnants of flight lines)
model1<-
kmeans(data.frame(ElevMax,ElevMean,ElevStdDev,ElevSkew,ElevKurtosis,Return3Above3,PercentAll
Above3,MaxHeight,P0to3,P3to6,P6to9,P9to12,P12to15,P15to18,P18to21,P21to24,P24to27,P27to30,P30t
o33), centers = 6, algorithm="Lloyd", iter.max=1000)

##Write k-means results to a file
write.matrix(model1,file="kmeans6.txt", sep =",")

##Read in k-means file
kmeans6<-scan("kmeans6.txt", what=numeric(), sep=",")

#Transpose the file from a row into a column
t(kmeans6)

##Add the clusters column to the data
data$Clusters6<-kmeans

##Write the data including k-means clusters to a file
write.table(unclass(data), "OSBSclusters6.txt", sep=",", col.names=T, row.names=F)
```

```
##segregate rows by cluster
data.sub1<-subset(osclusters, Cluster6==1)
write.table(unclass(data.sub1), "OSclustersSub6-1-1.txt", sep=",", col.names=T, row.names=F)

data.sub2<-subset(osclusters, Cluster6==2)
write.table(unclass(data.sub2), "OSBSclustersSub6-1-2.txt", sep=",", col.names=T, row.names=F)

data.sub3<-subset(osclusters, Cluster6==3)
write.table(unclass(data.sub3), "OSBSclustersSub6-1-3.txt", sep=",", col.names=T, row.names=F)

data.sub4<-subset(osclusters, Cluster6==4)
write.table(unclass(data.sub4), "OSBSclustersSub6-1-4.txt", sep=",", col.names=T, row.names=F)

data.sub5<-subset(osclusters, Cluster6==5)
write.table(unclass(data.sub5), "OSBSclustersSub6-1-5.txt", sep=",", col.names=T, row.names=F)

data.sub6<-subset(osclusters, Cluster6==6)
write.table(unclass(data.sub6), "OSBSclustersSub6-5-6.txt", sep=",", col.names=T, row.names=F)

##randomly select sites from the subsets, extra sites were selected to ensure that there were enough sites
within the boundaries of Ordway-Swisher
random1<-data.sub1[sample(nrow(data.sub1), 30), ]
random2<-data.sub2[sample(nrow(data.sub2), 30), ]
random3<-data.sub3[sample(nrow(data.sub3), 30), ]
random4<-data.sub4[sample(nrow(data.sub4), 30), ]
random5<-data.sub5[sample(nrow(data.sub5), 30), ]
random6<-data.sub6[sample(nrow(data.sub6), 30), ]

##write random samples to a table
write.table(unclass(random1), "OSRandom6-1-1.txt", sep=",", col.names=T, row.names=F)
write.table(unclass(random2), "OSRandom6-1-2.txt", sep=",", col.names=T, row.names=F)
write.table(unclass(random3), "OSRandom6-1-3.txt", sep=",", col.names=T, row.names=F)
write.table(unclass(random4), "OSRandom6-1-4.txt", sep=",", col.names=T, row.names=F)
write.table(unclass(random5), "OSRandom6-1-5.txt", sep=",", col.names=T, row.names=F)
write.table(unclass(random6), "OSRandom6-1-6.txt", sep=",", col.names=T, row.names=F)
```

Model Selection

```
setwd("G:/Thesis/Data")

##Read and attach the data
bat.data<-read.csv("BatMasterDataFINALworking2.csv",header=T)
names(bat.data)
bat<-subset(bat.data,ShanBatDiv != 0)
```

```
##Call package for AIC comparisons
library(AICcmodavg)

##Set up variable for diversity
Bat.Div<-bat$ShanBatDiv

##Normalize model parameters
vifCanMean<-bat$CanMean-mean(bat$CanMean)
vifEntropy<-bat$Entropy-mean(bat$Entropy)
vifRugosity<-bat$Rugosity-mean(bat$Rugosity)
vifProp015<-bat$Prop015-mean(bat$Prop015)
vifProp156<-bat$Prop156-mean(bat$Prop156)
vifProp612<-bat$Prop612-mean(bat$Prop612)
vifLandHeterogeneityerogeneity<-bat$LandHeterogeneity-mean(bat$LandHeterogeneity)
vifPropUrban<-bat$PropUrban-mean(bat$PropUrban)
vifPercentWater<-bat$AreaWater-mean(bat$AreaWater)
vifRoadLength<-bat$RoadLength-mean(bat$RoadLength)

##Log transform diversity data
logbat<-log(Bat.Div)

##models
cand.models<-list()

cand.models[[1]]<-
lm(logbat~vifCanMean+vifEntropy+vifRugosity+vifProp015+vifProp156+vifProp612, data=bat)
cand.models[[2]]<-
lm(logbat~vifCanMean*vifEntropy+vifRugosity+vifProp015+vifProp156+vifProp612, data=bat)
cand.models[[3]]<-lm(logbat~vifCanMean+vifEntropy+vifRugosity, data=bat)
cand.models[[4]]<-lm(logbat~vifCanMean*vifEntropy+vifRugosity, data=bat)

##2) Land heterogeneity will relate to bat community diversity

cand.models[[5]]<-
lm(logbat~vifCanMean+vifEntropy+vifRugosity+vifProp015+vifProp156+vifProp612+vifLandHeteroge
neity, data=bat)
cand.models[[6]]<-
lm(logbat~vifCanMean*vifEntropy+vifRugosity+vifProp015+vifProp156+vifProp612+vifLandHeteroge
neity, data=bat)

##3) Stand-level attributes will relate to bat community diversity
```

```
cand.models[[7]]<-
lm(logbat~vifCanMean+vifEntropy+vifRugosity+vifProp015+vifProp156+vifProp612+vifPropUrban+vif
PercentWater+vifRoadLength+vifLandHeterogeneity, data=bat)
cand.models[[8]]<-lm(logbat~
vifCanMean+vifEntropy+vifRugosity+vifProp015+vifProp156+vifProp612+vifPropUrban*vifLandHeter
ogeneity+vifPercentWater+vifRoadLength,data=bat)
cand.models[[9]]<-
lm(logbat~vifCanMean+vifEntropy+vifRugosity+vifProp015+vifProp156+vifProp612+vifPropUrban+vif
LandHeterogeneity*vifPercentWater+vifRoadLength,data=bat)
cand.models[[10]]<-
lm(logbat~vifCanMean+vifEntropy+vifRugosity+vifProp015+vifProp156+vifProp612+vifPropUrban+vif
PercentWater+vifRoadLength*vifLandHeterogeneity,data=bat)

##Create a vector of names to trace back models in set
modelnames<-paste("Model", 1:length(cand.models), sep=" ")

##Generate AICc table
aictab(cand.set=cand.models, modnames=modelnames, sort=TRUE)

##Set up variable for presence
labo<-bat.data$LABOPres

##models
labo.models<-list()

##1) Stand-level attributes will contribute to bat diversity. Expected contributions would be canopy
height, entropy, rugosity, and proportion of returns in height bins.

labo.models[[1]]<-glm(labo~CanMean+Entropy+Rugosity+Prop015+Prop156+Prop612,    data=bat.data,
family=binomial)
labo.models[[2]]<-glm(labo~CanMean*Entropy+Rugosity+Prop015+Prop156+Prop612,    data=bat.data,
family=binomial)
labo.models[[3]]<-glm(labo~CanMean+Entropy+Rugosity, data=bat.data, family=binomial)
labo.models[[4]]<-glm(labo~CanMean*Entropy+Rugosity, data=bat.data, family=binomial)

##2) Land heterogeneity will relate to bat community diversity

labo.models[[5]]<-
glm(labo~CanMean+Entropy+Rugosity+Prop015+Prop156+Prop612+LandHeterogeneity,  data=bat.data,
family=binomial)
labo.models[[6]]<-
glm(labo~CanMean*Entropy+Rugosity+Prop015+Prop156+Prop612+LandHeterogeneity,  data=bat.data,
family=binomial)
```

```
##3) Stand-level attributes will relate to bat community diversity

labo.models[[7]]<-
glm(labo~CanMean+Entropy+Rugosity+Prop015+Prop156+Prop612+PropUrban+AreaWater+RoadLength+LandHeterogeneity, data=bat.data, family=binomial)
labo.models[[8]]<-
glm(labo~CanMean+Entropy+Rugosity+Prop015+Prop156+Prop612+PropUrban*LandHeterogeneity+AreaWater+RoadLength,data=bat.data, family=binomial)
labo.models[[9]]<-
glm(labo~CanMean+Entropy+Rugosity+Prop015+Prop156+Prop612+PropUrban+LandHeterogeneity*AreaWater+RoadLength,data=bat.data, family=binomial)
labo.models[[10]]<-
glm(labo~CanMean+Entropy+Rugosity+Prop015+Prop156+Prop612+PropUrban+AreaWater+RoadLength*LandHeterogeneity,data=bat.data, family=binomial)

##Create a vector of names to trace back models in set
modelnames<-paste("Model", 1:length(labo.models), sep=" ")

##Generate AICc table
aictab(cand.set=labo.models, modnames=modelnames, sort=TRUE)

##Set up variable for presence
pesu<-bat.data$PESUPres

##models
pesu.models<-list()

##1) Stand-level attributes will contribute to bat diversity. Expected contributions would be canopy height, entropy, rugosity, and proportion of returns in height bins.

pesu.models[[1]]<-glm(pesu~CanMean+Entropy+Rugosity+Prop015+Prop156+Prop612,  data=bat.data, family=binomial)
pesu.models[[2]]<-glm(pesu~CanMean*Entropy+Rugosity+Prop015+Prop156+Prop612,  data=bat.data, family=binomial)
pesu.models[[3]]<-glm(pesu~CanMean+Entropy+Rugosity, data=bat.data, family=binomial)
pesu.models[[4]]<-glm(pesu~CanMean*Entropy+Rugosity, data=bat.data, family=binomial)

##2) Land heterogeneity will relate to bat community diversity

pesu.models[[5]]<-
glm(pesu~CanMean+Entropy+Rugosity+Prop015+Prop156+Prop612+LandHeterogeneity,  data=bat.data, family=binomial)
```

```
pesu.models[[6]]<-
glm(pesu~CanMean*Entropy+Rugosity+Prop015+Prop156+Prop612+LandHeterogeneity,  data=bat.data,
family=binomial)

##3) Stand-level attributes will relate to bat community diversity

pesu.models[[7]]<-
glm(pesu~CanMean+Entropy+Rugosity+Prop015+Prop156+Prop612+PropUrban+AreaWater+RoadLen
gth+LandHeterogeneity, data=bat.data, family=binomial)
pesu.models[[8]]<-
glm(pesu~CanMean+Entropy+Rugosity+Prop015+Prop156+Prop612+PropUrban*LandHeterogeneity+A
reaWater+RoadLength,data=bat.data, family=binomial)
pesu.models[[9]]<-
glm(pesu~CanMean+Entropy+Rugosity+Prop015+Prop156+Prop612+PropUrban+LandHeterogeneity*A
reaWater+RoadLength,data=bat.data, family=binomial)
pesu.models[[10]]<-
glm(pesu~CanMean+Entropy+Rugosity+Prop015+Prop156+Prop612+PropUrban+AreaWater+RoadLen
gth*LandHeterogeneity,data=bat.data, family=binomial)

##Create a vector of names to trace back models in set
modelnames<-paste("Model", 1:length(pesu.models), sep=" ")

##Generate AICc table
aictab(cand.set=pesu.models, modnames=modelnames, sort=TRUE)

##Set up variable for presence
laci<-bat.data$LACIPres

##models
laci.models<-list()

##1) Stand-level attributes will contribute to bat diversity. Expected contributions would be canopy
height, entropy, rugosity, and proportion of returns in height bins.

laci.models[[1]]<-glm(laci~CanMean+Entropy+Rugosity+Prop015+Prop156+Prop612,      data=bat.data,
family=binomial)
laci.models[[2]]<-glm(laci~CanMean*Entropy+Rugosity+Prop015+Prop156+Prop612,      data=bat.data,
family=binomial)
laci.models[[3]]<-glm(laci~CanMean+Entropy+Rugosity, data=bat.data, family=binomial)
laci.models[[4]]<-glm(laci~CanMean*Entropy+Rugosity, data=bat.data, family=binomial)

##2) Land heterogeneity will relate to bat community diversity
```

```
laci.models[[5]]<-
glm(laci~CanMean+Entropy+Rugosity+Prop015+Prop156+Prop612+LandHeterogeneity,  data=bat.data,
family=binomial)
laci.models[[6]]<-
glm(laci~CanMean*Entropy+Rugosity+Prop015+Prop156+Prop612+LandHeterogeneity,  data=bat.data,
family=binomial)

##3) Stand-level attributes will relate to bat community diversity

laci.models[[7]]<-
glm(laci~CanMean+Entropy+Rugosity+Prop015+Prop156+Prop612+PropUrban+AreaWater+RoadLengt
h+LandHeterogeneity, data=bat.data, family=binomial)
laci.models[[8]]<-
glm(laci~CanMean+Entropy+Rugosity+Prop015+Prop156+Prop612+PropUrban*LandHeterogeneity+Ar
eaWater+RoadLength,data=bat.data, family=binomial)
laci.models[[9]]<-
glm(laci~CanMean+Entropy+Rugosity+Prop015+Prop156+Prop612+PropUrban+LandHeterogeneity*Ar
eaWater+RoadLength,data=bat.data, family=binomial)
laci.models[[10]]<-
glm(laci~CanMean+Entropy+Rugosity+Prop015+Prop156+Prop612+PropUrban+AreaWater+RoadLengt
h*LandHeterogeneity,data=bat.data, family=binomial)

##Create a vector of names to trace back models in set
modelnames<-paste("Model", 1:length(laci.models), sep=" ")

##Generate AICc table
aictab(cand.set=laci.models, modnames=modelnames, sort=TRUE)

##Set up variable for presence
epfu<-bat.data$EPFUPres

##models
epfu.models<-list()

##1) Stand-level attributes will contribute to bat diversity. Expected contributions would be canopy
height, entropy, rugosity, and proportion of returns in height bins.

epfu.models[[1]]<-glm(epfu~CanMean+Entropy+Rugosity+Prop015+Prop156+Prop612,  data=bat.data,
family=binomial)
epfu.models[[2]]<-glm(epfu~CanMean*Entropy+Rugosity+Prop015+Prop156+Prop612,  data=bat.data,
family=binomial)
epfu.models[[3]]<-glm(epfu~CanMean+Entropy+Rugosity, data=bat.data, family=binomial)
epfu.models[[4]]<-glm(epfu~CanMean*Entropy+Rugosity, data=bat.data, family=binomial)
```

```
##2) Land heterogeneity will relate to bat community diversity

epfu.models[[5]]<-
glm(epfu~CanMean+Entropy+Rugosity+Prop015+Prop156+Prop612+LandHeterogeneity,  data=bat.data,
family=binomial)
epfu.models[[6]]<-
glm(epfu~CanMean*Entropy+Rugosity+Prop015+Prop156+Prop612+LandHeterogeneity,  data=bat.data,
family=binomial)

##3) Stand-level attributes will relate to bat community diversity

epfu.models[[7]]<-
glm(epfu~CanMean+Entropy+Rugosity+Prop015+Prop156+Prop612+PropUrban+AreaWater+RoadLen
gth+LandHeterogeneity, data=bat.data, family=binomial)
epfu.models[[8]]<-
glm(epfu~CanMean+Entropy+Rugosity+Prop015+Prop156+Prop612+PropUrban*LandHeterogeneity+A
reaWater+RoadLength,data=bat.data, family=binomial)
epfu.models[[9]]<-
glm(epfu~CanMean+Entropy+Rugosity+Prop015+Prop156+Prop612+PropUrban+LandHeterogeneity*A
reaWater+RoadLength,data=bat.data, family=binomial)
epfu.models[[10]]<-
glm(epfu~CanMean+Entropy+Rugosity+Prop015+Prop156+Prop612+PropUrban+AreaWater+RoadLen
gth*LandHeterogeneity,data=bat.data, family=binomial)

##Create a vector of names to trace back models in set
modelnames<-paste("Model", 1:length(epfu.models), sep=" ")

##Generate AICc table
aictab(cand.set=epfu.models, modnames=modelnames, sort=TRUE)

##Set up variable for presence
myau<-bat.data$MYAUPres

##models
myau.models<-list()

##1) Stand-level attributes will contribute to bat diversity. Expected contributions would be canopy
height, entropy, rugosity, and proportion of returns in height bins.

myau.models[[1]]<-glm(myau~CanMean+Entropy+Rugosity+Prop015+Prop156+Prop612,
data=bat.data, family=binomial)
myau.models[[2]]<-glm(myau~CanMean*Entropy+Rugosity+Prop015+Prop156+Prop612, data=bat.data,
family=binomial)
myau.models[[3]]<-glm(myau~CanMean+Entropy+Rugosity, data=bat.data, family=binomial)
```

```
myau.models[[4]]<-glm(myau~CanMean*Entropy+Rugosity, data=bat.data, family=binomial)

##2) Land heterogeneity will relate to bat community diversity

myau.models[[5]]<-
glm(myau~CanMean+Entropy+Rugosity+Prop015+Prop156+Prop612+LandHeterogeneity,
data=bat.data, family=binomial)
myau.models[[6]]<-
glm(myau~CanMean*Entropy+Rugosity+Prop015+Prop156+Prop612+LandHeterogeneity,
data=bat.data, family=binomial)

##3) Stand-level attributes will relate to bat community diversity

myau.models[[7]]<-
glm(myau~CanMean+Entropy+Rugosity+Prop015+Prop156+Prop612+PropUrban+AreaWater+RoadLen
gth+LandHeterogeneity, data=bat.data, family=binomial)
myau.models[[8]]<-
glm(myau~CanMean+Entropy+Rugosity+Prop015+Prop156+Prop612+PropUrban*LandHeterogeneity+
AreaWater+RoadLength,data=bat.data, family=binomial)
myau.models[[9]]<-
glm(myau~CanMean+Entropy+Rugosity+Prop015+Prop156+Prop612+PropUrban+LandHeterogeneity*
AreaWater+RoadLength,data=bat.data, family=binomial)
myau.models[[10]]<-
glm(myau~CanMean+Entropy+Rugosity+Prop015+Prop156+Prop612+PropUrban+AreaWater+RoadLen
gth*LandHeterogeneity,data=bat.data, family=binomial)

##Create a vector of names to trace back models in set
modelnames<-paste("Model", 1:length(myau.models), sep=" ")

##Generate AICc table
aictab(cand.set=myau.models, modnames=modelnames, sort=TRUE)

##Set up variable for presence
nyhu<-bat.data$NYHUPres

##models
nyhu.models<-list()

##1) Stand-level attributes will contribute to bat diversity. Expected contributions would be canopy
height, entropy, rugosity, and proportion of returns in height bins.

nyhu.models[[1]]<-glm(nyhu~CanMean+Entropy+Rugosity+Prop015+Prop156+Prop612,  data=bat.data,
family=binomial)
```

```
nyhu.models[[2]]<-glm(nyhu~CanMean*Entropy+Rugosity+Prop015+Prop156+Prop612,   data=bat.data,
family=binomial)
nyhu.models[[3]]<-glm(nyhu~CanMean+Entropy+Rugosity, data=bat.data, family=binomial)
nyhu.models[[4]]<-glm(nyhu~CanMean*Entropy+Rugosity, data=bat.data, family=binomial)

##2) Land heterogeneity will relate to bat community diversity

nyhu.models[[5]]<-
glm(nyhu~CanMean+Entropy+Rugosity+Prop015+Prop156+Prop612+LandHeterogeneity, data=bat.data,
family=binomial)
nyhu.models[[6]]<-
glm(nyhu~CanMean*Entropy+Rugosity+Prop015+Prop156+Prop612+LandHeterogeneity, data=bat.data,
family=binomial)

##3) Stand-level attributes will relate to bat community diversity

nyhu.models[[7]]<-
glm(nyhu~CanMean+Entropy+Rugosity+Prop015+Prop156+Prop612+PropUrban+AreaWater+RoadLen
gth+LandHeterogeneity, data=bat.data, family=binomial)
nyhu.models[[8]]<-
glm(nyhu~CanMean+Entropy+Rugosity+Prop015+Prop156+Prop612+PropUrban*LandHeterogeneity+
AreaWater+RoadLength,data=bat.data, family=binomial)
nyhu.models[[9]]<-
glm(nyhu~CanMean+Entropy+Rugosity+Prop015+Prop156+Prop612+PropUrban+LandHeterogeneity*
AreaWater+RoadLength,data=bat.data, family=binomial)
nyhu.models[[10]]<-
glm(nyhu~CanMean+Entropy+Rugosity+Prop015+Prop156+Prop612+PropUrban+AreaWater+RoadLen
gth*LandHeterogeneity,data=bat.data, family=binomial)

##Create a vector of names to trace back models in set
modelnames<-paste("Model", 1:length(nyhu.models), sep=" ")

##Generate AICc table
aictab(cand.set=nyhu.models, modnames=modelnames, sort=TRUE)

##models
negbinom.models<-list()

##1) Stand-level attributes will contribute to bat diversity. Expected contributions would be canopy
height, entropy, rugosity, and proportion of returns in height bins.

negbinom.models[[1]]<-glm.nb(total~CanMean+Entropy+Rugosity+Prop015+Prop156+Prop612,
data=bat.total)
```

```
negbinom.models[[2]]<-glm.nb(total~CanMean*Entropy+Rugosity+Prop015+Prop156+Prop612,
data=bat.total)
negbinom.models[[3]]<-glm.nb(total~CanMean+Entropy+Rugosity, data=bat.total)
negbinom.models[[4]]<-glm.nb(total~CanMean*Entropy+Rugosity, data=bat.total)

##2) Land heterogeneity will relate to bat community diversity

negbinom.models[[5]]<-
glm.nb(total~CanMean+Entropy+Prop015+Prop156+Prop612+LandHeterogeneity, data=bat.total)
negbinom.models[[6]]<-
glm.nb(total~CanMean*Entropy+Prop015+Prop156+Prop612+LandHeterogeneity, data=bat.total)
negbinom.models[[7]]<-
glm.nb(total~CanMean+Entropy+Rugosity+Prop015+Prop156+Prop612+LandHeterogeneity,
data=bat.total)

##3) Stand-level attributes will relate to bat community diversity

negbinom.models[[8]]<-
glm.nb(total~CanMean+Entropy+Rugosity+Prop015+Prop156+Prop612+PropUrban+AreaWater+RoadL
ength+LandHeterogeneity, data=bat.total)
negbinom.models[[9]]<-
glm.nb(total~CanMean+Entropy+Rugosity+Prop015+Prop156+Prop612+PropUrban*LandHeterogeneity
+AreaWater+RoadLength,data=bat.total)
negbinom.models[[10]]<-
glm.nb(total~CanMean+Entropy+Rugosity+Prop015+Prop156+Prop612+PropUrban+LandHeterogeneity
*AreaWater+RoadLength,data=bat.total)
negbinom.models[[11]]<-
glm.nb(total~CanMean+Entropy+Rugosity+Prop015+Prop156+Prop612+PropUrban+AreaWater+RoadL
ength*LandHeterogeneity,data=bat.total)

##Create a vector of names to trace back models in set
modelnames<-paste("Model", 1:length(negbinom.models), sep=" ")

##Generate AICc table
aictab(cand.set=negbinom.models, modnames=modelnames, sort=TRUE)
```

APPENDIX F: IACUC APPROVAL

University of Central Florida

Office of Research & Commercialization

12/2/2014

Dr. John Weishampel
Biology
BL 110
4000 Central FL Blvd
Orlando, FL 32816

Subject: Institutional Animal Care and Use Committee (IACUC) Protocol Submission

Dear Dr. John Weishampel:

This letter is to inform you that your following animal protocol was re-approved by the IACUC. The IACUC Animal Use Renewal Form is attached for your records.

Animal Project #:	13-38W
Title:	Acoustic surveying of bat community diversity in relation to LiDAR-derived forest structure
First Approval Date:	12/4/2013

Please be advised that IACUC approvals are limited to one year maximum. Should there be any technical or administrative changes to the approved protocol, they must be submitted in writing to the IACUC for approval. Changes should not be initiated until written IACUC approval is received. Adverse events should be reported to the IACUC as they occur. Furthermore, should there be a need to extend this protocol, a renewal must be submitted for approval at least three months prior to the anniversary date of the most recent approval. If the protocol is over three years old, it must be rewritten and submitted for IACUC review.

Should you have any questions, please do not hesitate to call the office of Animal Welfare at (407) 882-1164.

Please accept our best wishes for the success of your endeavors.

Best Regards,

Cristina Caamaño

Cristina Caamaño
Associate Director, Research Program Services

Copies: Facility Manager (when applicable.)

12201 Research Parkway • Suite 501 • Orlando, FL 32826-3246 • 407-823-3778 • Fax 407-823-3299

THE UNIVERSITY OF CENTRAL FLORIDA
INSTITUTIONAL ANIMAL CARE and USE COMMITTEE (IACUC)
Re-Approval to Use Animals

Dear Dr. John Weishampel,

Your application for IACUC Re-Approval has been reviewed and approved by the UCF IACUC Reviewers.

Approval Date: 12/1/2014

Title: Acoustic surveying of bat community diversity in relation to LiDAR-derived forest structure

Department: Biology

Animal Project #: 13-38W

Expiration: 12/4/2015

You may purchase and use animals according to the provisions outlined in the above referenced animal project. This project will expire as indicated above. You will be notified 2-3 months prior to your expriation date regarding your need to file another renewal.

Christopher Parkinson, Ph.D.
IACUC Chair

Approved ✓ Renewed ✓

LIST OF REFERENCES

Adams, A. M., Jantzen, M. K., Hamilton, R. M. , Fenton, M. B. (2012). Do you hear what I hear? Implications of detector selection for acoustic monitoring of bats. *Methods in Ecology and Evolution* 3, 992.

Agosta, S. J. (2002). Habitat use, diet and roost selection by the big brown bat (*Eptesicus fuscus*) in North America: A case for conserving an abundant species. *Mamm. Rev.* 32, 179.

Aldridge, H. D. J. N. , Rautenbach, I. L. (1987). Morphology, echolocation and resource partitioning in insectivorous bats. *J. Anim. Ecol.* 56, 763.

Angelo, J. J., Duncan, B. W. , Weishampel, J. F. (2010). Using LiDAR-derived vegetation profiles to predict time since fire in an oak scrub landscape in east-central Florida. *Remote Sensing* 2, 514.

Armitage, D. W. , Ober, H. K. (2012). The effects of prescribed fire on bat communities in the longleaf pine sandhills ecosystem. *J. Mammal.* 93, 102.

Arnett, E. B., Brown, W. K., Erickson, W. P., Fiedler, J. K., Hamilton, B. L., Henry, T. H., Jain, A., Johnson, G. D., Kerns, J., Koford, R. R., Nicholson, C. P., O'Connell, T. J., Piorkowski, M. D. , Tankersley, R. D. (2008). Patterns of bat fatalities at wind energy facilities in North America. *J. Wildl. Manage.* 72, 61.

Bender, M. J., Castleberry, S. B., Miller, D. A. , Wigley, T. B. (2015). Site occupancy of foraging bats on landscapes of managed pine forest. *For. Ecol. Manage.* 336, 1.

Bersier, L. F. , Meyer, D. R. (1994). Bird assemblages in mosaic forests - the relative importance of vegetation structure and floristic composition along the successional gradient. *Acta Oecologica-International Journal of Ecology* 15, 561.

Bestelmeyer, B. T. , Wiens, J. A. (2001). Ant biodiversity in semiarid landscape mosaics: The consequences of grazing vs. natural heterogeneity. *Ecol. Appl.* 11, 1123.

Bohm, S. M., Wells, K. , Kalko, E. K. V. (2011). Top-down control of herbivory by birds and bats in the canopy of temperate broad-leaved oaks (*Quercus robur*). *Plos One* 6.

Brigham, R. M. (1991). Flexibility in foraging and roosting behavior by the big brown bat (*Eptesicus fuscus*). *Canadian Journal of Zoology* 69.

Brigham, R. M., Grindal, S. D., Firman, M. C. , Morissette, J. L. (1997). The influence of structural clutter on activity patterns of insectivorous bats. *Canadian Journal of Zoology* 73, 131.

Britzke, E. R. (2014) Echoclass v 3.1. Retrieved from: http://www.fws.gov/midwest/Endangered/mammals/inba/surveys/inbaAcousticSoftware.html.

Burnham, K. P. , Anderson, D. R. (2002). *Model selection and multimodel inference: A practical information-theoretic approach*: Springer-Verlag.

Clawges, R., Vierling, K., Vierling, L. , Rowell, E. (2008). The use of airborne LiDAR to assess avian species diversity, density, and occurrence in a pine/aspen forest. *Remote Sens. Environ.* 112, 2064.

Corben, C. (2014) CFCRead Storage ZCAIM Interface version 4.4u. Retrieved from: www.hoarybat.com.

Davies, A. B. , Asner, G. P. (2014). Advances in animal ecology from 3D-LiDAR ecosystem mapping. *Trends Ecol. Evol.* 29, 681.

Docherty, M. , Leather, S. R. (1997). Structure and abundance of arachnid communities in scots and lodgepole pine plantations. *For. Ecol. Manage.* 95, 197.

Duchamp, J. E., Sparks, D. W. , Swihart, R. K. (2010). Exploring the "nutrient hot spot" hypothesis at trees used by bats. *J. Mammal.* 91, 48.

Environmental Systems Resource Institute. (2012) Arcmap 10.1. Redlands, CA. ESRI.

Farney, J. , Fleharty, E. D. (1969). Aspect ratio, loading, wing span and membrane areas of bats. *J. Mammal.* 50, 362.

Ford, M. (2014) Echolocation identification software results. Retrieved from: http://www.fws.gov/midwest/Endangered/mammals/inba/surveys/pdf/USGSTestReport1_201409015.pdf.

Ford, W. M., Menzel, M. A., Rodrigue, J. L., Menzel, J. M. , Johnson, J. B. (2005). Relating bat species presence to simple habitat measures in a central Appalachian forest. *Biol. Conserv.* 126, 528.

Frick, W. F., Pollock, J. F., Hicks, A. C., Langwig, K. E., Reynolds, D. S., Turner, G. G., Butchkoski, C. M. , Kunz, T. H. (2010). An emerging disease causes regional population collapse of a common North American bat species. *Science* 329, 679.

Goetz, S., Steinberg, D., Dubayah, R. , Blair, B. (2007). Laser remote sensing of canopy habitat heterogeneity as a predictor of bird species richness in an eastern temperate forest, USA. *Remote Sens. Environ.* 108, 254.

Grindal, S. D. , Brigham, R. M. (1999). Impacts of forest harvesting on habitat use by foraging insectivorous bats at different spatial scales. *Ecoscience* 6, 25.

Halaj, J., Ross, D. W. , Moldenke, A. R. (2000). Importance of habitat structure to the arthropod food-web in douglas-fir canopies. *Oikos* 90, 139.

Hein, C. D., Castleberry, S. B. , Miller, K. V. (2009). Site-occupancy of bats in relation to forested corridors. *For. Ecol. Manage.* 257, 1200.

Henry, M., Thomas, D. W., Vaudry, R. , Carrier, M. (2002). Foraging distances and home range of pregnant and lactating little brown bats (*Myotis lucifugus*). *J. Mammal.* 83, 767.

Hutchinson, J. T. , Lacki, M. J. (2000). Selection of day roosts by red bats in mixed mesophytic forests. *Journal of Wildlife Managemet* 64, 87.

Jones, G., Jacobs, D. S., Kunz, T. H., Willig, M. R. , Racey, P. A. (2009). Carpe noctem: The importance of bats as bioindicators. *Endangered Species Research* 8, 93.

Jost, L. (2006). Entropy and diversity. *Oikos* 113, 363.

Jung, K., Kaiser, S., Böhm, S., Nieschulze, J. , Kalko, E. K. V. (2012). Moving in three dimensions: Effects of structural complexity on occurrence and activity of insectivorous bats in managed forest stands. *J. Appl. Ecol.* 49, 523.

Lack, D. (1969). The numbers of bird species on islands. *Bird Study* 16, 193.

Lefsky, M. A., Cohen, W. B., Parker, G. G. , Harding, D. J. (2002). LiDAR remote sensing for ecosystem studies. *Bioscience* 52, 19.

Listopad, C. M. C. S., Masters, R. E., Drake, J. B., Weishampel, J. F. , Branquinho, C. (2015). Structural diversity indices based on ariborne LiDAR as ecological indicators for managing highly dynamic landscapes. *Ecol. Indicators* 57, 268.

Loeb, S. C. , O'Keefe, J. M. (2006). Habitat use by forest bats in South Carolina in relation to local, stand, and landscape characteristics. *Journal of Wildlife Managemet* 70, 1210.

MacArthur, R. H. (1958). Population ecology of some warblers of northeastern coniferous forests. *Ecology* 39, 599.

MacArthur, R. H. , MacArthur, J. W. (1961). On bird species diversity. *Ecology* 42, 594.

MacArthur, R. H. , Wilson, E. O. (1967). *The Theory of Island Biogeography*. Princeton: Princeton University Press.

Marciente, R., Brobrowiec, P. E. D. , Magnusson, W. E. (2015). Ground-vegetation clutter affects phyllostomid bat assemblage structure in lowland Amazonian forest. *PLoS One* 10, e0129560.

Marks, C., Marks, G. (2006). *Bats of Florida*. Florida: University Press of Florida.

Mazerolle, M. J. (2015) AICcmodavg: Model selection and multimodel inference based on (q)aic(c). R package version 2.0-3. Retrieved from: http://CRAN.R-project.org/package=AICcmodeavg.

McGaughey, R. J. (2014) Fusion/LDV and the LiDAR toolkit (LTK). Pacific Northwest Research Station. United States Department of Agriculture, Forest Service.

Menzel, J. M., Menzel, M. A., Kilgo, J. C., Ford, W. M. , Edwards, J. W. (2005a). Bat response to Carolina bays and wetland restoration in the southeastern U.S. Coastal Plain. *Wetlands* 25, 542.

Menzel, J. M., Menzel, M. A., Kilgo, J. C., Ford, W. M., Edwards, J. W. , McCracken, G. F. (2005b). Effect of habitat and foraging height on bat activity in the coastal plain of South Carolina. *Journal of Wildlife Managemet* 69, 235.

Merrick, M. J., Koprowski, J. L. , Wilcox, C. (2012). Into the third dimension: Benefits of incorporating LiDAR data in wildlife habitat models. In *7th Conference on Research and Resource management in the Southwester Deserts*: 389-395. Gottfried, G. J., Ffolliott, P. F., Gebow, B. S.,

Eskew, L. G., Collins, L. C. (Eds.). Tucson, AZ: United States Department of Agriculture, Forest Service, Rocky Mountain Research Station.

Mickelburg, S. P., Hutson, A. M. , Racey, P. A. (2002). A review of the global conservation status of bats. *Oryx* 36, 18.

Miller, D. A., Arnett, E. B. , Lacki, M. J. (2003). Habitat management for forest-roosting bats of North America: A critical review of habitat studies. *Wildl. Soc. Bull.* 31, 30.

Müller, J., Bae, S., Röder, J., Chao, A. , Didham, R. K. (2014). Airborne LiDAR reveals context dependence in the effects of canopy architecture on arthropod diversity. *For. Ecol. Manage.* 312, 129.

Muller, J. , Brandl, R. (2009). Assessing biodiversity by remote sensing in mountainous terrain: The potential of LiDAR to predict forest beetle assemblages. *J. Appl. Ecol.* 46, 897.

Noss, R. F. (1990). Indicators for monitoring biodiversity: A hierarchical approach. *Conserv. Biol.* 4, 355.

O'Farrell, M. J. (1998). A passive monitoring system from Anabat II using a laptop computer. *Bat Research News* 39, 147.

Ordway-Swisher Biological Station (2014) 2014 UF/IFAS Ordway-Swisher Biological Station Annual Report Retrieved from: http://ordway-swisher.ufl.edu/forms/14_OSBS_AR.pdf.

Palminteri, S., Powell, G. V. N., Asner, G. P. , Peres, C. A. (2012). Lidar measurements of canopy structure predict spatial distribution of a tropical mature forest primate. *Remote Sens. Environ.* 127, 98.

Patriquin, K. J. , Barclay, R. M. R. (2003). Foraging by bats in cleared, thinned and unharvested boreal forest. *J. Appl. Ecol.* 40, 646.

R Development Core Team. (2014) R: A language and environment for statistical computing. Vienna, Austria. R Foundation for Statistical Computing. Retrieved from: http://www.R-project.org.

Rainho, A., Augusto, A. M. , Palmeirim, J. M. (2010). Influence of vegetation clutter on the capacity of ground foraging bats to capture prey. *J. Appl. Ecol.* 47, 850.

Rainho, A. , Palmeirim, J. M. (2011). The importance of distance to resources in the spatial modelling of bat foraging habitat. *Plos One* 6, e19227.

Reutebuch, S. E., Andersen, H. E. , McGaughey, R. J. (2005). Light detection and ranging (LiDAR): An emerging tool for multiple resource inventory. *J. For.* 103, 286.

Schnitzler, H. U. , Kalko, E. K. V. (2001). Echolocation by insect-eating bats. *Bioscience* 51, 557.

Schwarzkopf, L. , Rylands, A. B. (1989). Primate species richness in relation to habitat structure in Amazonian rainforest fragments. *Biol. Conserv.* 48, 1.

Simmons, J. A., Fenton, M. B. , O'Farrell, M. J. (1979). Echolocation and pursuit of prey by bats. *Science* 203, 16.

Sleep, D. J. H. , Brigham, R. M. (2003). An experimental test of clutter tolerance in bats. *J. Mammal.* 84, 216.

Southwell, C. J., Cairns, S. C., Pople, A. R. , Delaney, R. (1999). Gradient analysis of macropod distribution in open forest and woodland of eastern Australia. *Aust. J. Ecol.* 24, 132.

Stephens, S. E., Koons, D. N., Rotella, J. J. , Willey, D. W. (2003). Effects of habitat fragmentation on avian nesting success: A review of the evidence at multiple spatial scales. *Biol. Conserv.* 115, 101.

U.S. Fish and Wildlife Service (2015). Indiana bat summer survey guidance.Retrived from: http://www.fws.gov/midwest/endangered/mammals/inba/inbasummersurveyguidance.html

Vallan, D. (2002). Effects of anthropogenic environmental changes on amphibian diversity in the rain forests of eastern Madagascar. *J. Trop. Ecol.* 18, 725.

Vierling, K. T., Bassler, C., Brandl, R., Vierling, L. A., Weiss, I. , Muller, J. (2011). Spinning a laser web: Predicting spider distributions using lidar. *Ecol. Appl.* 21, 577.

Waldon, J., Miller, B. W. , Miller, C. M. (2011). A model biodiversity monitoring protocol for REDD projects. *Tropical Conservation Science* 4, 254.

Wear, D. N. , Greis, J. G. (2002). Southern forest resource assessment - summary of findings. *J. For.* 100, 6.

Winhold, L., Kurta, A. , Foster, R. (2008). Long-term change in an assemblage of North American bats: Are eastern red bats declining? *Acta Chiropterol* 10, 359.